2019•2020

Faculteit Industriële ingenieurswetenschappen

master in de industriële wetenschappen: elektronica-ICT

Masterthesis

Innovative setup to measure bulk resistance in battery electrodes

PROMOTOR :

Prof. dr. Mohammadhosein SAFARI

BEGELEIDER :

De heer Hamid HAMED

Siebe Clerinx

Scriptie ingediend tot het behalen van de graad van master in de industriële wetenschappen: elektronica-ICT

Gezamenlijke opleiding UHasselt en KU Leuven

UHASSELT KU LEUVEN

UHASSELT KU LEUVEN

2019•2020

Faculteit Industriële ingenieurswetenschappen

master in de industriële wetenschappen: elektronica-ICT

Masterthesis

Innovative setup to measure bulk resistance in battery electrodes

PROMOTOR :

Prof. dr. Mohammadhosein SAFARI

BEGELEIDER :

De heer Hamid HAMED

Siebe Clerinx

Scriptie ingediend tot het behalen van de graad van master in de industriële wetenschappen: elektronica-ICT

UHASSELT

KU LEUVEN

Preface

With great pleasure I would like to present to you my master's thesis, which has been the final step towards my degree in Engineering Technology with specialization in Electronics and ICT. It have been a remarkable and exiting four and a half years that have built up to this. I look back proudly at what I have accomplished but I am also relieved to be able to close this chapter of my life. I can now look forward with excitement with what the future will bring.

First and foremost, I would like to thank my supervisor, mister Hamid Hamed, for putting with me for over a year and supporting me along the way. He was the first person I could go to whenever I had any question and from there he would set me on my way.

Furthermore I want to thank every person at UHasselt and IMO that has helped me out with all my experiments and during my trials and (more often than I would like to admit) errors.

Finally, I want to thank my friends and family for supporting me during this period. They were there when I was at the end of my rope and made sure I always retrieved my drive and continued on this endeavor.

Table of Contents

List of Figures

List of Tables

Abstract

A lithium ion battery's(LIB) performance is strongly affected by its effective transport properties including effective ionic conductivity and effective electronic conductivity. The electrode microstructure of a LIB is the most important factor in determining these effective properties in LIBs and is affected not only by the nature of electrode components, but also the manufacturing process.

The aim of this project is to design a novel setup to measure the effective electronic conductivity of lithium ion electrodes in order to gain more insight into the limiting factors that result in battery performance deterioration. The focus of this research lies on measuring bulk conductivity values and local electronic conductivity variations of cathode electrodes, as there is a lack of correlation between the reported measured electronic conductivity values and battery performance in current literature.

For this purpose, three different measuring probes were developed and tested: a Pogo Pin Probe, a 3D Printed Probe and a PCB Probe, the latter of which showed the most promising results of the three. It uses a micro four-line probe to measure a voltage drop caused by the resistance of the battery electrode, which is coated on top. The PCB has multiple of these four-line probes. By changing the probe combination, it is possible to determine spatial resistance differences over the electrode's surface and depth.

Abstract in het Nederlands

De prestatie van Lithium-ion batterij (LIB) is sterk afhankelijk van zijn transporteigenschappen, zoals ionische geleidbaarheid en elektronische geleidbaarheid. De microstructuur van de electrode van een LIB is een van de belangrijkste factoren in het bepalen van deze eigenschappen in LIB'en en hangt niet enkel af van de componenten van de elektrode, maar ook van het productieproces.

Het doel van dit project is het ontwerpen van een nieuwe opstelling om de elektronische geleidbaarheid van lithium-ion elektroden te meten en meer inzicht te krijgen in de limiterende factoren die de prestaties van een batterij doen verslechten. De focus van dit onderzoek ligt bij het meten van bulk conductiviteit en de lokale verschillen in elektronische geleidbaar van kathode elektrodes. Er is immers een tekort aan vergelijking tussen de gemeten elektronische geleidbaarheid en de prestaties van een batterij in de huidige literatuur.

Voor dit doel zijn er drie opstellingen ontwikkeld: een Pogo Pin Probe, een 3D-geprinte Probe en een PCB Probe, waarvan de laatste de meest veelbelovende is. De opstelling maakt gebruik van een micro vier-lijn probe om een spanningsverschil te meten, veroorzaakt door de weerstand van de batterijelectrode, die de bovenkant van de PCB bedekt. De PCB heeft meerdere van deze probes. Door de combinatie van probes te veranderen kunnen de ruimtelijke verschillen van de coating bepaalt kunnen worden, zowel over het oppervlak als in de diepte.

1. Introduction

Lithium ion battery (LIB) electrodes have a complicated porous structure and normally consist of a slurry made up of an active material, a conductive additive and a polymeric binder. The microstructural complexity comes from the interactions between the particles in these layers and has a major impact on the battery performance. These particle interactions are not only influenced by the nature of the components used in making the battery slurry, but also the manufacturing processes play a vital role in determining what will be the spatial location of the particles relative to each other. On the other hand, as the need for developing batteries with higher performance and better cycle life to meet energy storage requirements is increasing rapidly, it is of great interest to study how manufacturing processes can affect battery performance.

A typical LIB cell (besides housing parts), consist of two electrodes (cathode and anode) which are basically porous solid structures, a separator which is placed between the electrodes and prevents electrical contact and an electrolyte which fills the pores and facilitates ion transfer between the two electrodes. The electron transfer is supported by the electrode solid matrix which consists of conductive additives (most of the time the active material itself also has electronic conductivity to some extent).

According to the literature, there are two opposite schools of thoughts about the rate limitations controlling battery performance. The first one suggests that rapid electron transport (including short- and long-range contacts) governs the performance while the other one argues that tortuous ion pathways are the predominant factor controlling the rate capability. In order to gain more insight into this controversial problem and to study the electrode microstructure in detail, we will introduce a novel setup for measuring the through plane (bulk or volume) electronic conductivity variations of the LIB electrodes. We will also study how the conductivity is affected by the manufacturing process and how they will influence battery performance.

Current testing methods to measure battery performance are often limited to measuring the surface resistivity of a thin film solid electrolyte using a Four Point Probe (4PP). As mentioned before, it would be useful to determine the bulk resistivity of the film.

Bulk resistivity, measured in ohms-cm, gives the inherent resistance of a given material regardless of the shape or size [1]. The bulk resistivity can be calculated by multiplying the thickness of the layer in centimetres with the sheet resistance expressed in ohms per square. But when the thickness of the layer is unknown or hard to quantify accurately because the conductivity of the matrix is not isotropic, calculating the bulk resistance is not possible.

The new setup we are introducing will focus on establishing a way to measure the bulk resistivity of a thin film sample but is also aimed at determining conductivity differences in a single thin film electrode. Non-uniformities in the film lead to heterogeneous aging of the battery and consequently decrease the performance of a battery cell over its life cycle. Thus, developing a method to map the conductivity in different areas of the thin film can help advance production and application methods to get more uniform electrode layers.

In this study the composition and workings of a lithium-ion battery will be explained according to the way they are produced in the IMO laboratory.

After, different already existing measurement setups will be discussed, and their pros and cons compared. Here it will also be mentioned which aspects of other methods can be useful to incorporate in the new bulk resistivity measurement setup, what should be improved and what shows to be ineffective for the new use case.

Finally, the new bulk measurement setups are presented (as multiple were setups were developed and tested). The theoretical aspects behind the design choices are explained. The methods and materials used to manufacture the probe design and the measurement setup are clarified. The use of the setup is explained as well as the accompanying measurement results.

2. The Lithium-ion battery

The batteries produced in the IMO lab and used for testing in this report are lithium-ion batteries (LIBs). The primary components of a lithium-ion battery are the cathode (positive electrode), the anode (negative electrode) and an electrolyte, with a current collector on each of the electrodes.

The anode material is commonly made of a carbon-based material such as graphite, although lithium and other metals like copper can be used [2]. But due to graphite's optimal qualities such as structural stability, low electrochemical reactivity and lithium ion storage conditions, the material is considered suitable to be used for anodes [3]. The anode at IMO is made up of graphite, with a copper current collector.

The cathode consists of three main components: an active material, conductive carbon additives and a polymeric binder. The active material (of a lithium-ion battery) is commonly some lithium compound, like a combination of lithium and oxygen; lithium oxide [3]. At IMO, NMC or Lithium Nickel Cobalt Manganese Oxide ($\mathrm{LiNiCoMn}O_2$) is used. The added carbon particles are used to increase the conductivity. The polymeric binder acts as an adhesive which helps the active material and conductive carbon additive to adhere to the cathode substrate [3]. A solvent is needed to get the materials incorporated with each other. At IMO, this solvent is called NMP or N-Methyl-2-pyrrolidone (C_5H_9NO). Mixing the solvent with the other materials results in a slurry that can be coated onto the (aluminium) current collector to create the cathode electrode.

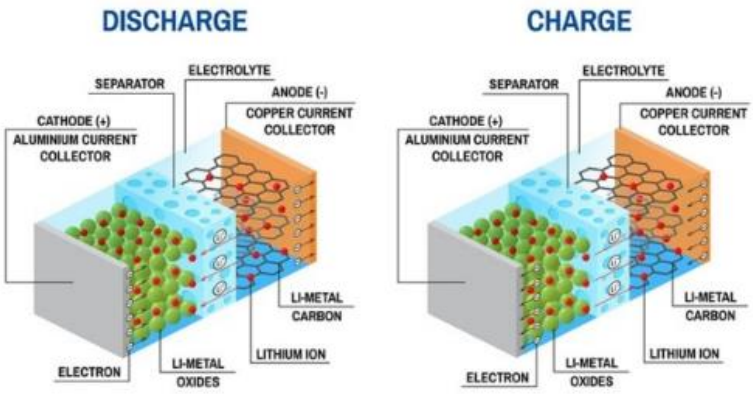

Figure 2.1: A Li-ion battery diagram [2]

A separator isolates the cathode from the anode. The separator is saturated with electrolyte and forms a catalyst that promotes the movement of ions from cathode to anode during charging and in the reverse direction when discharging, as can be seen in Figure 2.1. Although ions can freely move through the separator, it has no electrical conductivity of itself [4].

Charging and discharging of a lithium-ion battery goes as follows: during discharge, lithium ions (Li+) flow from the anode (negative electrode) to the cathode (positive electrode), through the electrolyte and separator diaphragm. The electrons will flow through an external circuit and supply a current from the battery to the desired component.
During charging, an over-voltage (a higher voltage than the battery produces) is applied using an external power source, forcing a charging current to flow within the battery from the positive to the negative electrode. The lithium ions then migrate back from the positive to the negative electrode, where they become embedded in the porous electrode (carbon) material. In a lithium-ion battery the lithium ions are transported to and from the positive or negative electrodes by oxidizing (loss of electrons) the transition metal during charge and reducing (gain of electrons) during discharge [5].

To create the desired thickness of the electrolyte layer, the materials are often deposited using physical vapour deposition (PVD) techniques such as sputtering and thermal evaporation [2]. Or, as

used in the IMO lab, a Thick Film Coater, which is designed to produce films with consistent thickness by using micrometre height adjustable applicators [6], and a calendaring device, where the film is passed through heated rollers to give it a homogenous finish. These techniques are cheaper but less accurate. Typical Li-ion battery electrodes have a film thickness on the order of 30 − 100µm.

3. The importance of electronic conductivity

The capacity of a battery is of limited significance if the battery cannot deliver the stored energy effectively. For this to be true, batteries also need low internal resistance. Since a more conductive battery can deliver stored energy more effectively, can charge faster and lasts longer, it is important that research is conducted into developing more conductive coatings [7]. Be it by finding new combinations for electrolyte coatings or by playing with the ratios of the coating components.

In theory, a battery is often represented as an ideal voltage source. This means that no matter what load is attached to the battery, the voltage at the source's terminals will always stay the same. In reality, several factors can limit a battery's ability to act as an ideal voltage source: battery size, chemical properties, age and temperature all affect the amount of current a battery can source. Then, a more practical model would be that of an ideal voltage source in series with a resistor, indicating the internal resistance of the battery.
Thus, the internal resistance of a battery depends on its size, chemical properties, age, temperature, and the discharge current it is subjected to. Because the voltage at the source's terminals will not be ideal due to the factors mentioned before, this affects the amount of current a battery is able to source [8]. High resistance can also cause a battery to heat up and the voltage to drop under load, triggering an early shutdown [9].
Battery resistance is the result of the electronic resistivity of the component materials of the battery and ionic resistance due to electrochemical factors such as electrolyte conductivity, ion mobility, and electrode surface area [10]. The internal resistance of Li-ion cells also increases with use and age, as the battery components degrade [9].

If internal resistance is a limiting factor of a battery's overall performance, better conductance will allow for better battery performance. Battery conductance describes the ability of a battery to transmit current through its internal electro-chemical structure [11] [12]. More conductivity leads to better rate capability of a cell and a uniform distribution of the conductive matrix across the electrode is needed for homogenous aging of the cell. A non-uniform distribution of this matrix results in heterogeneous aging, which is an undesirable effect. Thus, electronic conductivity is an important aspect of battery technology to research and improve.

4. Existing measurement setups

4.1. Four-Point Probe

The Four-Point Probe (4PP) setup is one of the most widely used apparatus for the measurement of resistivity of semiconductors [13]. The 4PP method is used to measure the surface resistivity of a sample. Sheet resistance is expressed as “ohms-per-square”.

The probe consists of four equally spaced (*s* in Figure 4.1) metal tips with a finite radius, arranged in a straight line, as can be seen in Figure 4.1. Each tip can be supported by springs as to minimize sample damage during probing. The four tips can travel up and down to make contact with the conducting film (blue rectangle in Figure 4.1). Evidently, the sample size should be greater than the length of the probe.

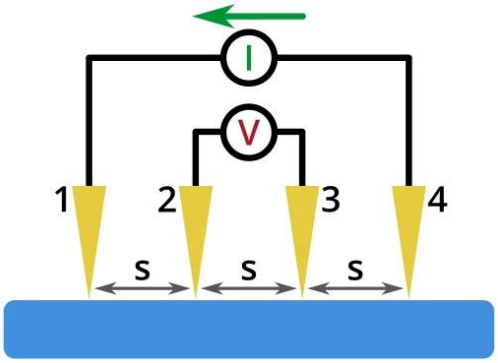

Figure 4.1: Schematic diagram of a four-point probe [14]

The 4PP operates by applying a current (*I*) onto the outer two probes (numbered 1 and 4) and measuring the resulting voltage drop between the inner two probes (numbered 2 and 3). In case the material being tested is no thicker than 40% of the spacing *s* and the sample is significantly (typically 40 times larger) than the spacing of the probes , the sheet resistance (R_s) can then be calculated using the equation below [14]:

$$R_s = \frac{\pi}{ln(2)} * \frac{\Delta V}{I}$$

$with$:
$I = applied\ current$
$\Delta V = measured\ voltage\ drop$

$\frac{\pi}{\ln(2)} = standard\ geometric\ correction\ factor\ for\ a\ semi - infinite\ thin\ sheet\ (also\ named\ Van\ der\ Pauw\ constant)$ [15]

If the previously named requirement is not met, then geometric correction factors are needed which account for the size, shape, and thickness of the sample. To correct for geometric factors, the measured sheet resistance is multiplied by the proper factor to get the correct value for the sample.

The correction factor for circular samples can be calculated using following formula:

$$C = \frac{\ln(2)}{\ln(2) + \ln\left(\frac{d^2}{s^2} + 3\right) - \ln\left(\frac{d^2}{s^2} - 3\right)}$$

For rectangular samples, there is no equation and instead a table of empirical correction factors is used and depend on the width *b* and length *a* of the sample and the spacing of the probes *s* [14] [16].

$R(\frac{b}{s}, \frac{a}{b})$

$\frac{b}{s}$	$\frac{a}{b} = 1$	$\frac{a}{b} = 2$	$\frac{a}{b} = 3$	$\frac{a}{b} \geq 4$
1			0,2204	0,2205
1,25			0,2751	0,2751
1,5		0,3263	0,3286	0,3286
1,75		0,3794	0,3803	0,3803
2		0,4292	0,4297	0,4297
2,5		0,5192	0,5194	0,5194
3	0,5422	0,5957	0,5958	0,5958
4	0,6870	0,7115	0,7115	0,7115
5	0,7744	0,7887	0,7888	0,7888
7,5	0,8846	0,8905	0,8905	0,8905
10	0,9313	0,9345	0,9345	0,9345
15	0,9682	0,9696	0,9696	0,9696
20	0,9822	0,9830	0,9830	0,9830
40	0,9955	0,9957	0,9957	0,9957
∞	1	1	1	1

Figure 4.2: Correction factors for a thin, rectangular sample. Thickness $< \frac{s}{2}$, s = probe spacing, a = width, b = length (long side) [13, p. 54]

The values in this table only apply when the probes make contact in the centre of the sample, and are aligned parallel to the sample's long edge (b, see Figure 4.2).
Reference work [16] provides the correction factors and explanation for the previously mentioned geometries as well as many others, like bulk samples where the film thickness is much greater than the probe spacing.

One of the primary advantages of using a 4PP is the elimination of the lead or wire resistance (this is the resistance of a connection between electrically connected locations) and contact resistance (resistance due to surface conditions and other causes, when contacting interfaces of electrical leads and connections are touching one another) to the sample. Separation of current and voltage electrodes eliminates those parasitic resistances [14], [17], [18].
The applied current I enters and leaves the sample via the outer probes and flows through the sample. Voltmeters typically have a high electrical impedance to prevent them affecting the circuit being measured, so no current will flow through the inner two probes. Thus, only the voltage between the inner probes is measured, meaning that the wire resistances and the contact resistances do not contribute to the measurement. The only voltage decrease that will be measured is the one caused by the sample resistance itself.

If the thickness of the sample film is known, the volume resistivity (in ohms-cm) can be calculated by multiplying the sheet resistance by the thickness of the coating in centimetres [1]. The problem with this approach is that the surfaces of materials can often have significantly lower surface resistivity than the bulk, due to defects or other contaminations. Measurements using the techniques described above then give falsely low values for the bulk resistivity [19].

4.2. Four-Line Probe

The Four-Line Probe technique is an extension of the 4PP concept. A line probe uses parallel lines to contact the sample instead of points. Compared to a point probe, a line probe increases the contact area with the thin film and enhances the stability between the probe and the sample [17].

[20] describes a micro four-line probe that can be precisely replaced onto the sample using actuators. With each replacement, a new measurement can be conducted, thus creating a map of the conductivity and the contact resistance.

4.3. Powder Probe

With a Powder Contact Probe, it is possible to eliminate parasitic electrical losses that occur when a rigid contact medium (like a probe) is applied to a (microscopically) rough surface.
A Powder Probe uses stainless steel particles attached to a magnet. The magnet is used as a probe and the particles serve as contact media to the sample. The collective of particles feature high plasticity and thus conform to the topography of the surface of the sample when pressed down onto the sample. In contrast to other setups, it is the contact media that is deformed instead of the sample. This results in a non-destructive measurement setup [18]. The coupling can be optimized by indenting the surface of the electrode like is done with the 4PP. This will result in the thin film being deformed plastically and the electrical connection between the stamp and the conductive layer will be improved. However, this deformation can cause changes in the electrical properties of the electrode.

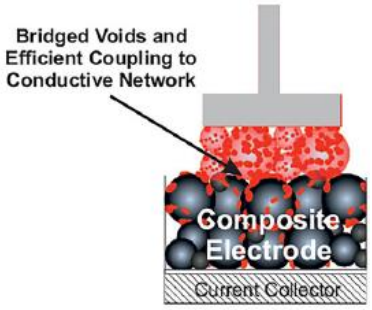

Figure 4.3: Powder probe with particles (red spheres) attached to a magnetic mount [15, p. 1551]

4.4. Electrochemical Impedance Spectroscopy

Electrochemical Impedance Spectroscopy (EIS) is a method that is used to study a systems response to the application of a periodic small-amplitude AC signal, over a range of frequencies.
The result of EIS is the impedance of the electrochemical system as a function of the frequency [21]. Impedance indicates the opposition to the flow of an alternating current (AC) in a complex system. If a system is purely resistive (this is, no complex component), then the opposition to AC or direct current (DC) is simply the resistance. Most physico-chemical systems (including electrochemical cells), materials or systems exhibiting multiple phases (such as composites or heterogeneous materials) possess energy storage and dissipation properties. These systems show a universal dielectric response (dielectric meaning the system can be polarized by applying an electric field, universal response meaning the behaviour of the dielectric properties can be observed in most solid-state systems), whereby EIS reveals a relationship between the impedance (or admittance) and the frequency of the applied AC field [22].

As mentioned, electrochemical impedance is usually measured by applying a small excitation AC potential. The response to this potential is an AC current signal. This current signal can be measured and analysed as a sum of sinusoidal functions (a Fourier series).
By using a small excitation signal, the cell's response is pseudo-linear. In linear and pseudo-linear systems, the current response to a sinusoidal potential will be a sinusoid with the same frequency but shifted in phase. The impedance is therefore expressed in terms of magnitude (Z_0) and phase shift (Φ) [23].
Data from an EIS measurement can then be represented in a Bode and Nyquist plot. In these plots the impedance can be split up in a real and imaginary part and describes their relation between frequency and magnitude or phase [24].
Analysis of this system response reveals information about the interface, its structure, the reactions taking place as well as energy storage and dissipation properties of the cell [25].

5. Methods & Materials

In what follows, there will be a discussion of three different probing setups that were designed, constructed and tested. For each setup the underlying theoretical aspects will be explained. Then there is a detailed description of the fabrication process of the setups. This includes both commentary on the materials used and their significance as well as an explanation of the fabrication methods of each process.

All setups are designed with the same requirements in mind: a setup has to be able to measure bulk resistivity, map local differences in a sample, be cost effective, easy to produce (mostly considering the production time) and be easy to use. The contact resistance between the probes and the sample had to be minimized by coating the slurry directly onto the probes. This enables another set of probes to function as top probes to send a current through the cathode laminate and measure the voltage difference in the same manner as with the 4PP method.

After discussing the setups, there is an explanation of the measuring device and software that is used to get measurements with the probes.

5.1. Setup 1: Pogo pin probe

The first developed setup consists of following elements:

The sample, consisting of a *probing pattern* applied to a *glass substrate* and coated with the cathode electrode.

The probe contacts the sample via *pogo pins* and is used to guide currents to and receive voltages from the sample. The pins are placed onto a *PCB* made for making easy connections to the probes on the sample. Everything is placed into an acrylic *enclosure*. A pressure sensor allows the user to control the pressure of the pogos onto the sample. This prevents damaging the sample and allows for measurements in function of a certain applied pressure.

5.1.1. Probing pattern & sample preparation

The probing pattern is based on a new four-point probe design as can be found in the literature [26] and is a variation on the usual four-point probe.
The pattern is made in such a way that there are rectangular pads lying outside of the coating. They are used to make contact with the measuring probes. Via a thin path these pads are connected to other circular pads. These pads take on the function of points for a four-point measurement. From the outer pads, the current will flow from one pad to the other. The inner pads are used to measure a voltage difference.
The pads described above can only be used to conduct surface measurements. To be able to get bulk measurements, there have to be contacts on top of the coating as well. For this, the pattern needs to be below and on top of the coating. So, the sample is prepared as shown in Figure 5.1.
The contacts on top of the probe as can be seen in Figure 5.1c, are made using pins that contact that side of the coating (see 5.1.2.1).

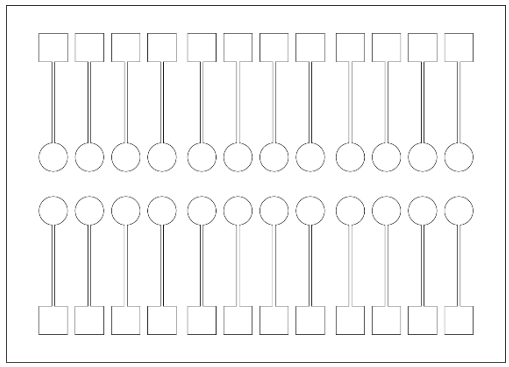

Figure 5.2: Probe CAD drawing. Used to cut a mask that is used to metal sputter the pattern onto a substrate.

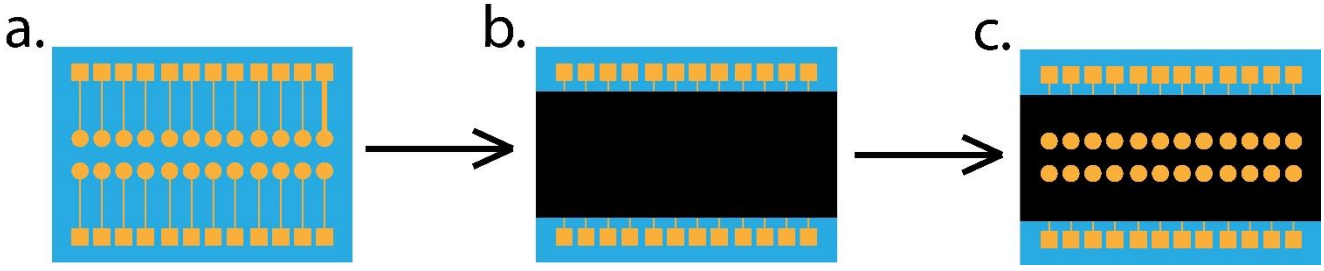

Figure 5.1: Diagram of sample preparation for bulk measurement.
In a. the probing pattern is applied to a glass substrate.
In b. the cathode electrolyte is coated onto the pattern, leaving the rectangular pads exposed.
Finally, in c. it is indicated where the probes would contact on the other side of the coating (aligned with the underlaying probes).

Two different methods were explored to deposit the pattern onto the substrate: sputter deposition and printing.

The pattern was designed using AutoCAD Mechanical, a mechanical design software by Autodesk used for manufacturing [27].

5.1.1.1. Sputter deposition

Sputter deposition is a physical vapor deposition (PVD) method. It aims at depositing a thin film of material onto a target. First, the source material is subjected to a gas plasma (often Argon is used, as it is an inert gas that cannot chemically combine with other atoms or compounds [28]). The energetic atoms of the plasma collide with the target material and knock off source atoms. The knocked off source atoms then travel to the substrate under the influence of an electric field and condense into a thin film [29], [30].

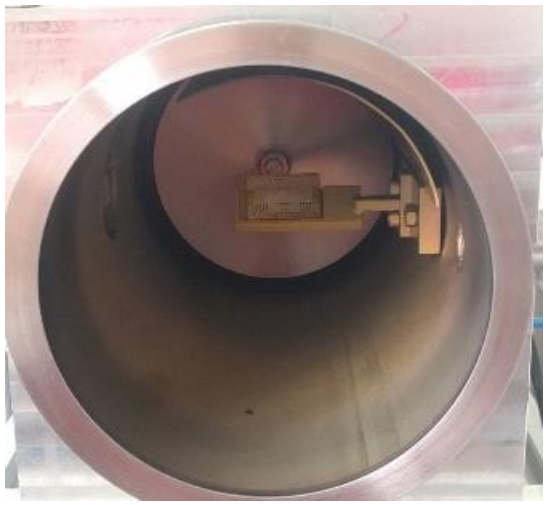

Figure 5.3: Sputtering machine at IMO. A substrate with mask is placed in the socket.

Using a mask on top of the target substrate, part of the substrate is shielded from the source atoms and thus a pattern can be created. In this case, the mask is made out of an aluminium sheet with a thickness of 0.1mm. The pattern was cut out using a laser cutter. The source materials used were gold and titanium. First, a thin layer of titanium was deposited and finished with depositing gold.

Before deposition can start, the substrate on which to coat (in this use case glass) must be thoroughly cleaned. The sample is submerged in acetone and then in ethanol for 10 to 15 minutes each. After that, UV-ozone treatment is performed on the substrate. This removes organic residue contaminants from the substrates and improves adhesion of the source material to the substrate. The ozone treatment uses two wavelengths of UV light (185 and 254 nm). 185-nm UV light dissociates molecular oxygen (O_2) into triplet atomic oxygen. This triplet oxygen then reacts with another O_2 molecule to form ozone. Next, the 254nm UV light dissociates the ozone molecules. This results in the formation of O_2 and singlet atomic oxygen. Singlet oxygen has strong oxidation properties and it will react with organic materials present on the samples surface. The singlet oxygen will cause chain scission of these organic materials and they will be transformed into harmless by-products such as CO_2, H_2O and O_2 [31].

After, the sample is loaded into the sputtering machine and the sputtering process can start.

5.1.1.2. Metal Printing

The second method that was explored was metal printing. There is no need for a mask, as a drawing of the desired pattern can be uploaded straight to the printer. Silver printer ink was used for the samples because it was readily available in the lab. The sample can be prepared in the same was a in 5.1.1.1, but cleaning the substrate with ethanol or acetone should be sufficient.

5.1.2. Probing

To probe a prepared sample, pogo pins are used. The pogo pins will contact the probing pattern and the coating. The pogos are fixed to a printed circuit board that also provides the needed connections to hook the setup up to a measuring device. A pressure sensor is present to control the applied force to the sample. Everything is brought together in an acrylic enclosure.

5.1.2.1. Pogo pins

Pogo pins are electrical connectors with a spring-loaded mechanism and are used in many modern electronic applications and in the electronics testing industry [32]. Pogos are useful thanks to their spring mechanism. It makes sure that all the probes contact the sample, even if they are not perfectly level with each other. The pogos used in the setup are Smiths Interconnect Contact Probes (GSS-100 Series) [33] with a flat tip style.
All the tips are soldered to a custom PCB which is designed to guide currents and voltages to and from a standard pin header for easy connections.

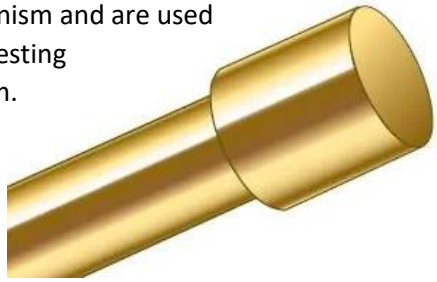

Figure 5.4: Smiths Interconnect Contact Probes with flat tip [33, p. 1].

5.1.3. Printed Circuit Board

The PCBs of this setup was designed using the Eagle PCB Design Software by Autodesk. Two PCBs were developed: one for solely surface resistivity measurements (probes on one side of the electrode coating) and one for bulk measurements (probes on both sides of the coating). The PCBs are milled from a copper plate (single sided copper for the Surface PCB, double sided for the Bulk PCB) using the PCB mill in the PXL Makerspace. The pogo pins are soldered to the PCB and copper traces connect them to male breakout pins. Each row of four pins can be used to conduct a measurement.

The Surface PCB was made simply to confirm the operation of the setup, as it was easier to design and produce since it was a single sided PCB.

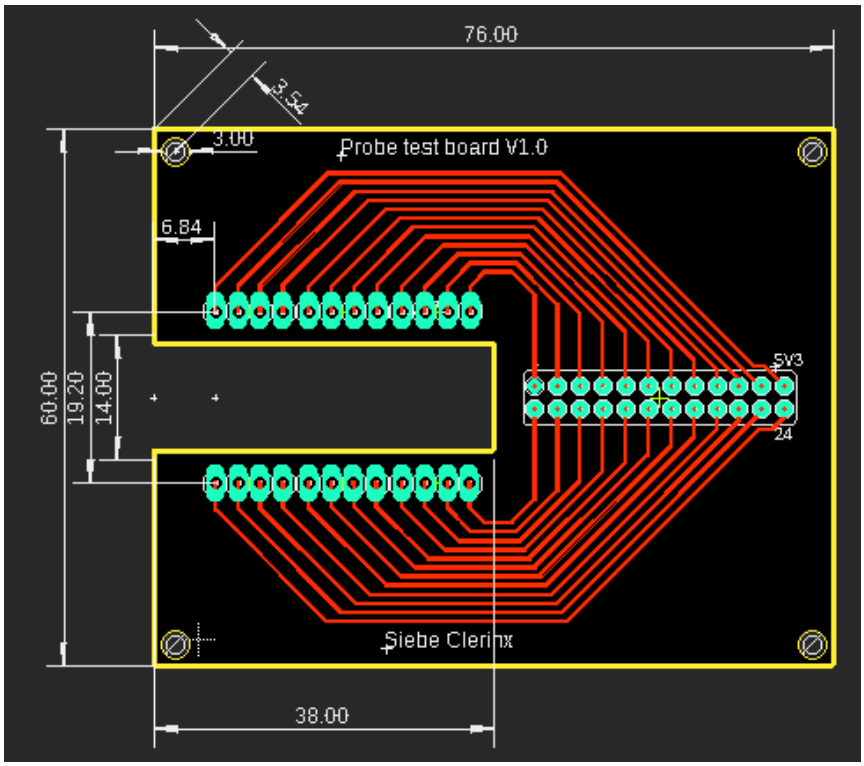

Figure 5.5: PCB board view for surface resistivity measurements (also Surface PCB))

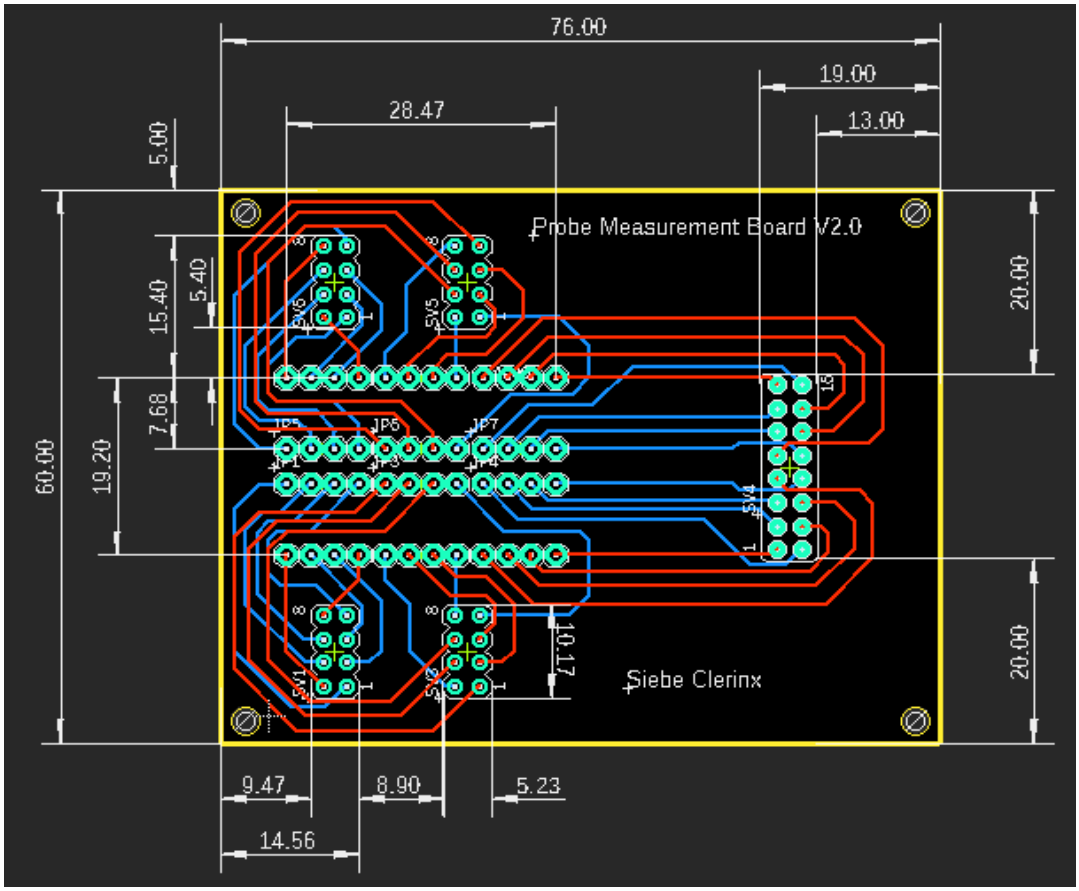

Figure 5.6: PCB board view for bulk resistivity measurements (also Bulk PCB)

5.1.4. Probe Enclosure

The acrylic holder makes sure the sample stays in place and that the probes on the sample line up with the pins on the board. The bottom plate supports the sample and the pressure sensor (see 5.1.5). Next is a plate with a cavity for the pressure sensor. Following that, the holder has recesses for the sample and the breakout pins. On top of the holder, the circuit board is placed. The top plate protects the board and has recesses for the breakout pins as well as the pogo pins.

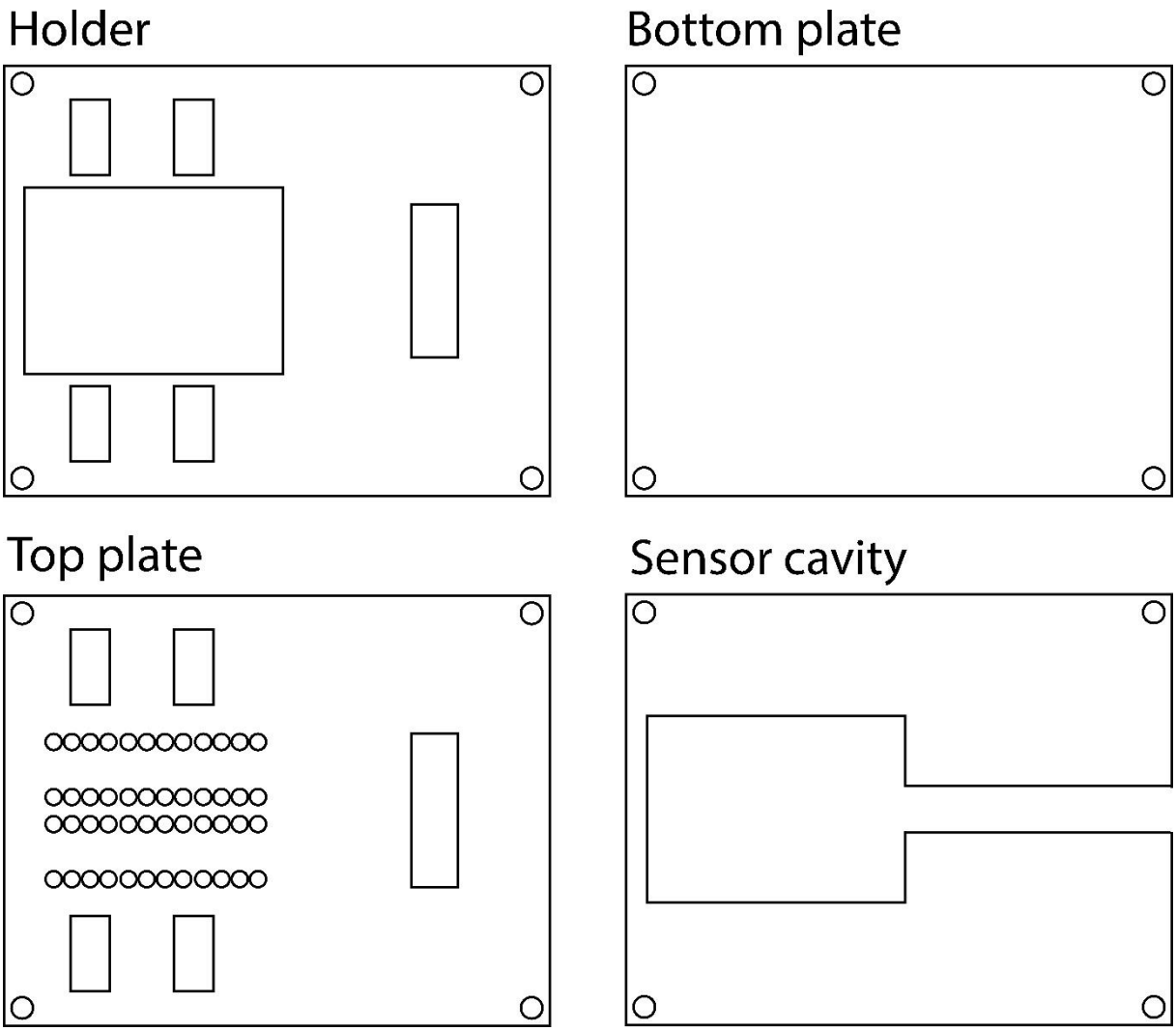

Figure 5.7: Diagram of the PCB holder

The drawings in Figure 5.7 were created using Adobe Illustrator. Acrylic plates with a thickness of 2 and 3 millimetre were laser cut using the laser cutter present at the PXL Makerspace.
The acrylic plates and the circuit board are fixed together with four 2cm bolts to bring the setup together.

5.1.5. Pressure Sensor

To avoid damaging the sample when loading it into the holder and fixing it in place, a pressure sensor was added. The sensor is a FlexiForce Pressure Sensor made by Tekscan [34]. It is a piezoresistive force sensor. Such sensors are based on the piezoresistive effect. This effect describes a change in the electrical resistivity of a semiconductor or a metal when mechanical strain is applied. The greater the strain, the lower the sensor's resistance. When no force is applied, the resistance will be infinite.
To read out the sensor, a voltage divider is used.
A voltage divider is a circuit which turns a large voltage into a smaller one, using two resistors in series and an input voltage. This will generate a variable voltage output, which can be read by a microcontroller's ADC (Analog to Digital Converter) input [35].

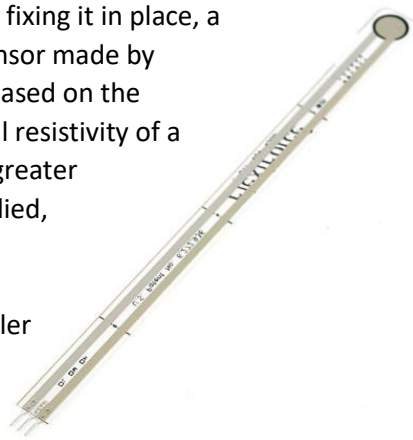

Figure 5.8: FlexiForce Pressure Sensor [34]

The output voltage can be calculated using following equation:

$$V_{out} = V_{in} \frac{R_2}{R_1 + R_2}$$

with R_1 *the variable resistance of the sensor*
R_2 *a fixed resistance*

Using these values, the applied pressure to the sample can be controlled.

The sensor data is acquired using an Arduino microcontroller. The hook-up will be as follows (see Figure 5.9): one sensor pin is connected to the 5V rail, the other to an analogue pin (for sensor readout). The fixed-value resistor is connected to ground [36]. The read-out values are show on a seven-segment display. The values are also logged in the build-in serial monitor of the Arduino IDE. The data is properly formatted so it can be easily copied into a spreadsheet program.

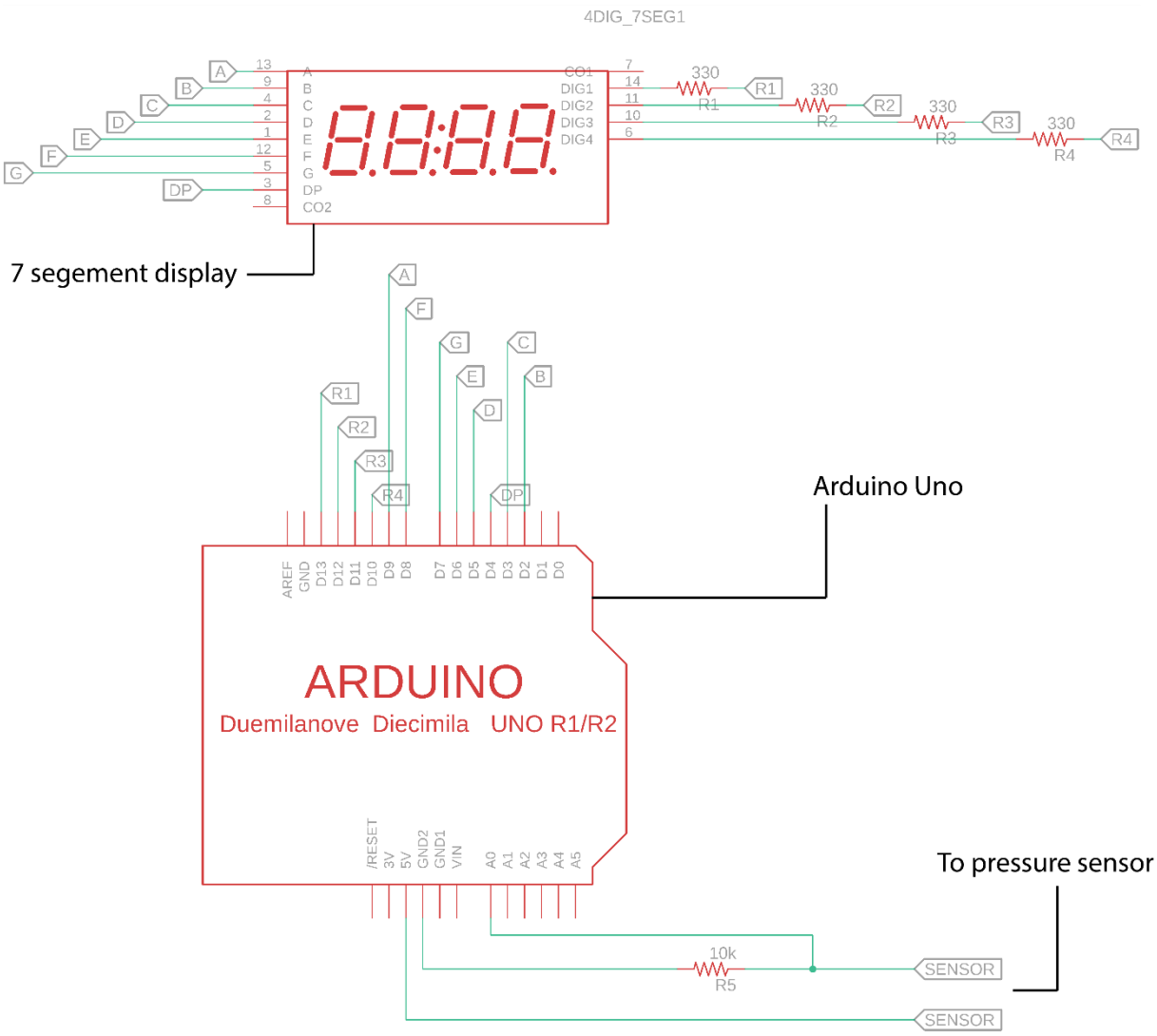

Figure 5.9: Pressure sensor and display schematic

The sample is placed on top of the sensor when tightening the plates of the holder. This way the pressure can be monitored and controlled.

5.2. Setup 2: 3D Printed probe

This second setup was developed having the micro-four-line probe as seen in [20] in mind. It consists of following components:

The 3D prints, for both the top and bottom probe, made using a resin printer. The prints are coated with a metal *ink* to create the probing pattern and electrical contacts.

The mask needed to coat the ink in the right pattern onto the 3D prints. A technique called "*screen printing*" is used.

5.2.1. Probing Pattern

As mentioned earlier, the probe and by extend the geometry of the probing pattern are based on the micro four-line probe shown in [20]. There it is stated that, as a general rule, the distance between the outer lines of the probe should approximate the thickness of the film. Because of technical limitations (explained later), the lines were designed to be 250µm wide and 3mm long, with 250µm spacing between the lines. This pattern is repeated five times on an approximately 1,52cm² area (1,175cm by 1,3cm). This is done so that later on during measuring, the conductance differences in different places of the coating can be examined. The mentioned line pattern is extended and gradually widened to provide places for electrical contacts to use as measuring points (see Figure 5.10: CAD drawing of the bottom probe mask & Figure 5.11: 3D CAD Models of the bottom probe (top left), top probe (top right) and representation of the compound setup (bottom)).

The pattern can be found both on the top and bottom 3D prints.

5.2.2. Mask

A mask is used to coat the ink onto the print and create the desired pattern, using a method called screen printing. The mask is made out of a sheet of 0,1mm thick aluminium. The template for this pattern was drawn using AutoCAD Mechanical. The pattern is cut into the aluminium sheet using the laser cutter present at the PXL Makerspace. As can be seen in Figure 5.10: CAD drawing of the bottom probe mask, in yellow there are some rectangular pads. These are used to be able to contact the probes of the top substrate. The pads will be on both the top and bottom substrate and this way will make an electrical contact when the ink patterns are applied.

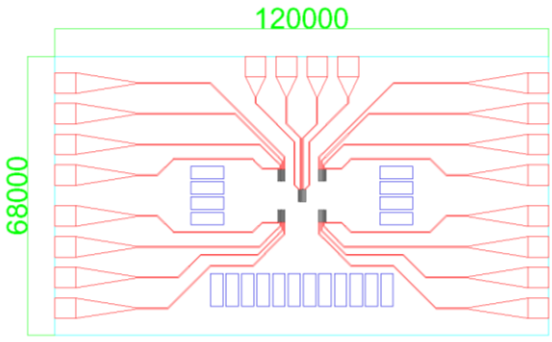

Figure 5.10: CAD drawing of the bottom probe mask

When wanting to coat a print, one must take into account that the mask and the print need to be aligned perfectly on top of each other, as the 250µm wide lines of the print and the mask can easily be misaligned.

5.2.3. 3D Printed Substrate

The 3D prints serve as the substrate for the probe and the coat. First, the complete pattern of the bottom and top probe were drawn using the same AutoCAD drawing from the mask described in the previous section. Then this design was imported into Fusion360 in order to create a 3D model.

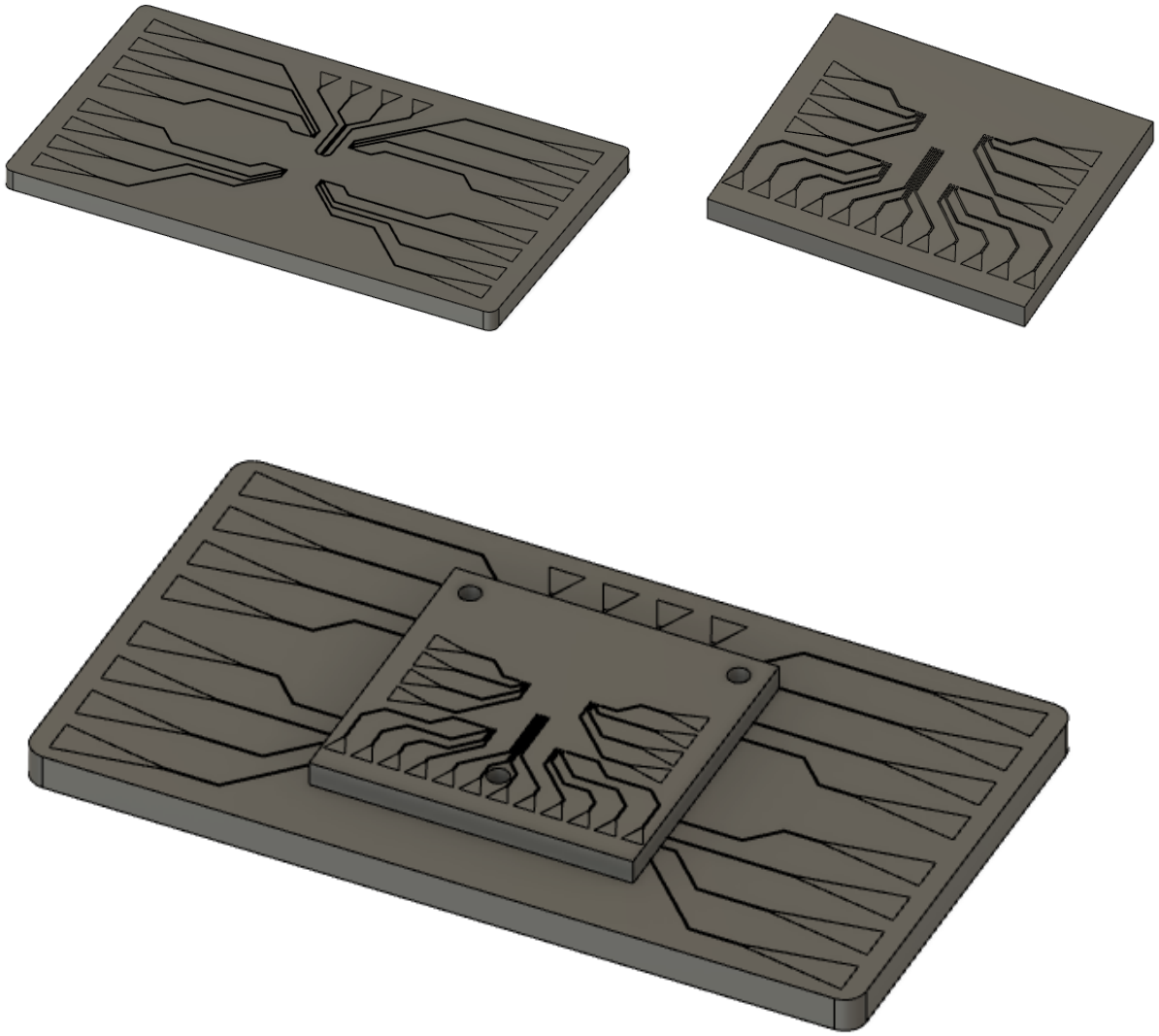

Figure 5.11: 3D CAD Models of the bottom probe (top left), top probe (top right) and representation of the compound setup (bottom)

Because the setup exists of two probes that are placed on top of each other, it must be prevented that the respective patterns do not interfere with each other. To achieve this, the prints have grooves in which the electrical contacts will be. The grooves are 50µm deep, which is greater than the thickness of the ink coating (see 5.2.4.2 for values of the layer thickness of tested inks).

As the pattern is on a micrometre scale, a 3D printer that could reach this accuracy had to be used. The printer used is the Original Prusa SL1, made by Prusa Research, as it can reach a minimum layer height of 0.01mm (10µm), though 0.025mm is the recommended height for optimal results. Considering this recommended resolution, it was decided to have the channels be 50µm deep.

The Prusa SL1 is able to reach this level of accuracy because it is based on the Masked Stereolithography (MSLA) process [37]. SLA printers are made up of a vat of a photo-reactive liquid and a light source. The liquid contains monomers and when exposed to light, the monomers link together to form polymers [38]. These polymers are solid. This way, very thin layers can be formed. By selectively exposing the liquid (according to the desired design), one solid 3D object can be created.

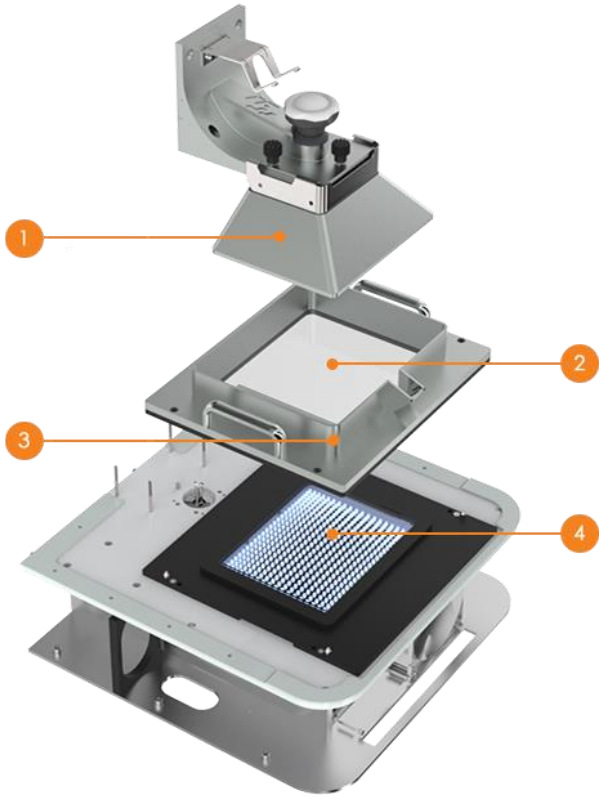

Figure 5.13: Diagram of the Original Prusa SL1 with (1) Build platform, (2) Digital LCD mask, (3) Resin container, (4) LED array [68]

MSLA utilizes an LED array as its light source together with an LCD photomask in order to shape the light image from the LED array. The LCD photomask digitally displays the layer pattern. To create a layer in the resin, individual pixels of the LCD are deactivated to allow light from the LED array to pass through, which cures the resin. This technique makes MSLA more accurate than a DLP-SLA. The DLP variant uses a digital light projector (DLP). Here, the resolution depends on how well the lens of the projector is focused, while with MSLA, the resolution only depends on the resolution of the LCD photomask [39] [40].

The resin used in the SL1 is a photopolymer though resin, sold by Prusa Research [41]. This resin is UV sensitive [42] and is specifically made for printing objects where toughness and durability are important [41]. The resin is composed of epoxy resin (reactive polymers), monomers, photoinitiators and colour pigment. To get a finished product, the resin has to be hardened through a process called curing where the resin changes its properties. The properties of the photopolymers (also known as light-activated resin) change when exposed to (ultraviolet) light. Photoinitiators in the resin decompose in reactive species, like free radicals, anions or cations, when affected by radiation. These released reactive species activate polymerization of the monomers and polymers in the resin. They cross-link with each other which causes the resin to harden [41] [42] [43]. The composition of the resin must be

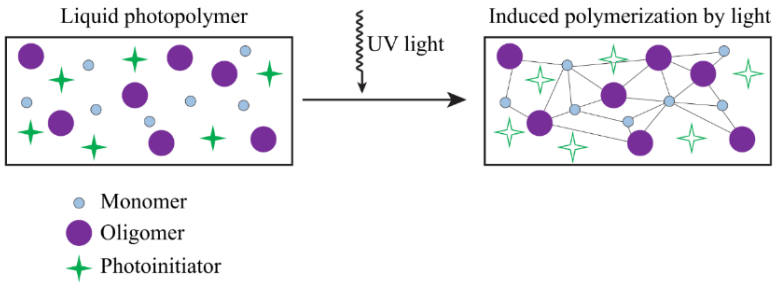

Figure 5.12: Curing process of a liquid photopolymer [43]

carefully balanced to meet the requirements of the cured product, in this case a hard and durable end product [44].

5.2.4. Ink Coating

The material used for screen printing the probing pattern is a silver metal ink. Multiple inks were tested on different criteria before choosing an appropriate ink that suited the needs the most.

5.2.4.1. Ink Criteria

For choosing the right ink, different criteria that had to be met were presupposed. This list of criteria was composed with the ideas of creating a robust probe that can be used multiple times without having to replace the probing pattern. It also has to meet electrical and physical expectations.

The criteria are:

- Curing temperature

Each ink contains solvents to hold metal particles and create a paste that can be spread out to create a coat. After coating, those solvents need to be evaporated. This can be done using an oven or a high-powered light source. As the ink is coated on a resin substrate, the temperature during curing should not exceed the glass transition temperature. This is the temperature region where polymers transition from a hard material to a soft, rubbery material [45]. Thus, reaching this temperature can deform the substrate and subsequently screw up the whole setup. If the transition temperature of the resin was not disclosed in its datasheet, it was a matter of empirical testing to check if the substrate was deformed in any way after curing.
Each ink was cured using a combination of two heat treatments: first, the ink was exposed to a pulsating near infrared light. Locally, this will heat up the ink to 150°C, melt the silver particles and fuse them together after cooling. Next, the ink was put into an oven at 90°C for about 15 minutes.

- Layer thickness

The layer thickness is important as it cannot be greater than the 50µm grooves present in the 3D substrate. After curing of the ink, when the metal particles have fused and the solvents have evaporated, it must be made sure that the layer thickness does not exceed this limit.

- Particle size

The size of the metal particles in the ink are important. The particle size cannot be greater than the geometry of the mask and substrate.

- Electrical resistance

The influence of resistance of the probe compared to that of the electrode coating should be reduced as much as possible. Thus, it would be favourable to select an ink with a small or neglectable electrical resistance.

- Adhesion to substrate

Because a lot of time would be lost if the probing pattern has to be reprinted after each use, the ink needs to adhere well to the surface of the substrate. Preferred is an ink that does not come loose when handling the substrate, scratching the surface or rubbing it with a cloth or paper towel.

- Resistance to chemicals (notably acetone and ethanol)

The battery electrode coating that will cover the probe can be removed with acetone or ethanol. For the same reason as stated in the previous section, the ink should be resistant to at least one of those chemicals.

5.2.4.2. Tested inks

The criteria mentioned in the previous chapter were tested on four different inks:

- AGFA Orgacon Nanosilver Screen Printing Ink Si-P2000

This is a highly conductive silver ink for printed electronics applications, specifically on flexible substrates. The film thickness of this ink when printed and cured is 1-2µm, with a resolution of 150µm (for lines). The recommended curing cycle is 10 minutes at 150°C but higher temperatures and longer times will yield lower sheet resistance. The maximum curing temperature is rated at 250°C. The volume resistivity of the ink amounts to 3mΩ/□/25µm (with 25µm the DFT or Dry Film Thickness). Thinning is done with Butyl Cellosolve™ (2-Butoxyethanol). The clean-up solvent is butyl diglycol acetate or similar [46].

- Loctite ECI 1011 E&C

This Loctite ink is a screen printable silver ink with high electrical conductivity. It is an ink used for paper and PET substrates and high frequency applications. The particle size of this ink amounts to less than 2µm. The recommended drying cycle is 10 minutes at 150°C. The sheet resistance of this ink is less than 5mΩ/□/25µm. Loctite can reach a line count of 50 lines per centimetre or 200µm per line [47].

- Gwent Group Flexible Silver Paste C2131014D3

This ink is a heat curable paste designed for use in electro luminescent systems. It is designed for a low temperature curing process. It has good chemical and environmental resistance properties.

- Gwent Group Flexible Silver Paste C2090210D12

No datasheet was available for this ink as it is pulled from the market. From other sources, like [48], the curing conditions can be found to be 130 ℃ for 3 minutes. In an experiment conducted in [49], the conditions were 120 °C for 4.5 minutes. As stated on multiple datasheets (including the ones of the ink described above), the drying profile may vary based on customers' experience, application requirements (e.g. layer thickness), equipment and environmental conditions.

5.2.5. Screen Printing

To transfer the ink onto the substrate, a technique called screen printing was used. Screen printing is a printing technique where a mesh is used to transfer ink onto a substrate, except in areas made impermeable to the ink by a blocking mask. A blade or squeegee is moved across the screen to fill the mesh with ink. A reverse stroke causes the screen to touch the substrate. This causes the ink to wet the substrate and be pulled out of the mesh as the screen springs back after the blade has passed [50]. Originally, a mesh screen would be ordered. But the cost of a screen with the desired resolution was too great to justify. In reaction to this, a mask (as described in 5.2.2) was used instead.

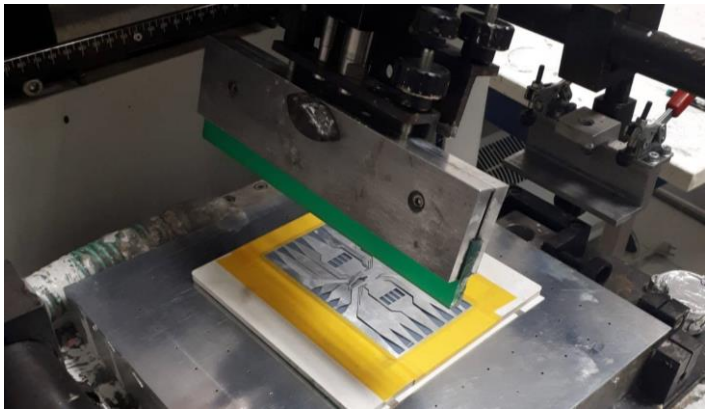

Figure 5.15: Screen printing setup with squeegee (in green)

In this use case, the substrate is place in a 3D printed holder. Then, the mask is carefully aligned with the substrate. Next, everything is fixed using tape. Now the ink can be deposited lengthwise of the substrate and the squeegee can be moved across the mask to fill the gaps with ink (see Figure 5.14).

Figure 5.14: Screen printing procedure

5.3. Setup 3: PCB Probe

The third and final setup that will be presented is a probe made from printed circuit boards (PCBs). The probe pattern is also made according to the four-line probe in [20]. This setup consists of the following components:

Two PCBs, one for a bottom probe and one for a top probe. The boards can be clamped together and will sandwich the coating. Each board has pin header connections to hook it up to a measuring device.

5.3.1. Probing Pattern

The 4-line pattern that is exposed by the solder mask can be seen in Figure 5.16.
As can be observed, each line has a width of 250µm. The lines are spaced 250µm from one another. The length of each line is 3.5mm. At each end there is a rounded tip with a height of 110µm.

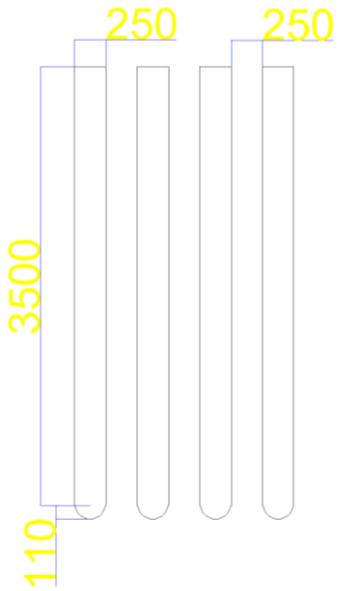

Figure 5.16: Dimensions (in µm) of probing pattern of the PCB probe

5.3.2. Printed Circuit Boards

As mentioned before, two printed circuit boards were designed. The boards were designed using Autodesk EAGLE (Easily Applicable Graphical Layout Editor) software. EAGLE is an electronic design automation program developed by Autodesk. It has features for schematic design and PCB layout and allows to connect schematic diagrams, components placement and PCB routing [51] [52].
Each PCB has the same line pattern (inspired by [20]). Again, like in the previous setup, the pattern is repeated multiple times. Later, the regional differences in the coating can be determined.
When the PCBs are placed on top of each other, the lines will align above each other. To prevent the copper traces of the PCBs from touching each other during contact, a solder mask was applied. A solder mask is a protective layer applied to a printed circuit board. It protects the copper from oxidation, environment and short circuits [53]. At the necessary places, the solder mask was omitted. For example, the mask is not present where the four line probe should be exposed to allow for a current flow between the lines. The mask was also removed on the pads where the headers are soldered, which is standard practice for places where components have to be soldered to the board. The boards can be clamped together using 3mm diameter screws as each board has four drill holes. The bottom PCB has dimensions of 15cm by 15cm. This PCB is made large enough so the header pins do not obstruct the coating process. The top probe is 5cm by 9cm. As can be seen, the top probe has copper on both sides of the PCB. Using through holes, the copper lines can be funnelled through the PCB to the other side. This way headers can be added and connected to the lines of the PCB. There is no need for weird contact areas between the top and bottom probe in order to ensure a connection like was necessary in 5.2. The PCBs were ordered at Eurocircuits, a Belgium based company with factories in Germany and Hungary [54].

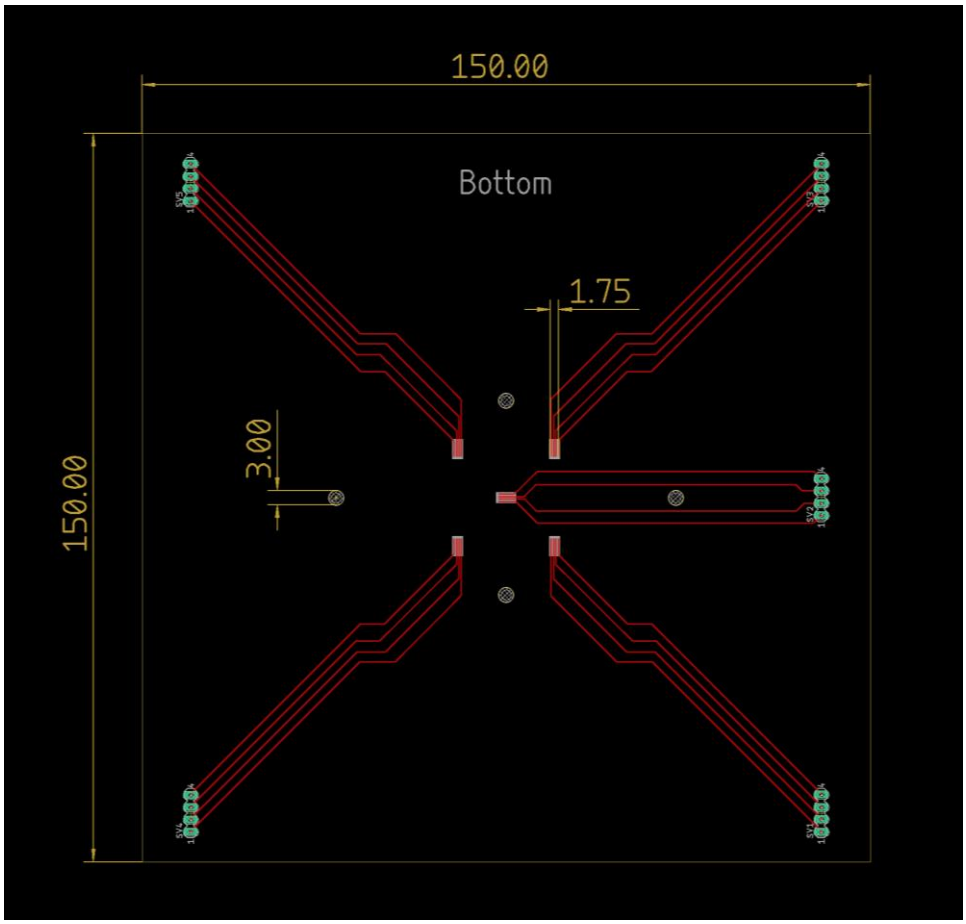

Figure 5.17: PCB Layout of bottom probe with in red the top copper

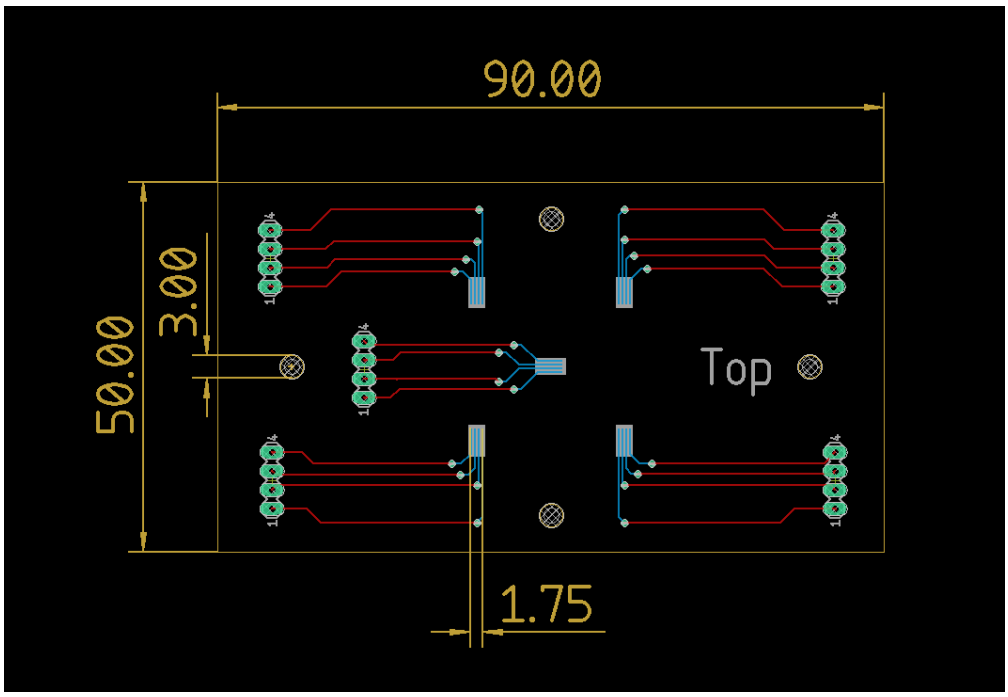

Figure 5.18: PCB Layout of top probe with in red the top copper and in blue the bottom copper

5.4. Measuring & Data Logging

To test a setup, preform measurements and get data, a device was needed that could send out a current and read back a corresponding voltage.
For this, an HTM four-wire sensing (four-point probe method) program together with a Keysight B2901A Precision Source/Measuring Unit or a Keithley 2400 and Keithley 2401 Source Meter/Unit (Figure 5.19). Both units were used, depending on which one was available at the lab. The unit can send out a precise current. Using a pair of electrodes, the current is supplied to two probes of the setup. Another electrode pair measures the voltage. The program converts the measured voltage to a resistance using Ohms law ($R = \frac{U}{I}$) [55] [56]. Four-terminal sensing is an effective way to compensate voltage drops on low resistance paths, such as the current leads. It also eliminates parasitic resistances like lead and contact resistance from the measurement. This way, resistance of the electrodes is rejected, resulting in a more accurate measurement [57].
By placing the voltage measuring electrodes on the opposite side of the thin film in relation to the current leads, it can be observed how much current will travel through the bulk of the coating. This way the bulk resistance of the film can be determined.

The four wires that are connected to the Keysight Unit can be extended using male to female jumper wires. In turn, these can be connected using the female side of the wire to the headers present on the PCBs.

In the software, a current can be entered. Via the four-wire sensing, the software shows the measured voltage difference. It uses the applied current and measured voltage to calculate a resistance value. These values are plotted onto a live graph in the software. All data (voltage, current, resistance and other corresponding timestamp) is saved to a Comma Separated Value (CSV) file. This data can now be analyzed.

Figure 5.19: Keithley 2400 & Keithley 2401 Source Meter/Unit

6. Results & Discussion

In this section the outcome of each setup and its production will be presented and discussed. There will be explained what parts of a setup work and where the drawbacks lie.

The outcomes of sheet resistance and bulk resistance measurements will also be considered. They will be compared to theoretical and practical resistivity numbers as well as Ossila 4PP Sheet resistance measurements.

6.1. Setup 1: Pogo pin Probe

In what follows, the glass sample substrate and the applied probe are discussed. Next, the PCB and the setups enclosure are presented. Finally, the results from conduction measurements with the setup are cited.

6.1.1. Sample

While producing a usable sample, several drawback and limitations emerged when using the sputtering method.

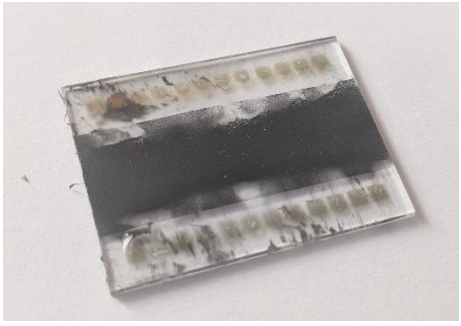

Figure 6.1: Prepared sample after use

The first drawback is that the sample production is time consuming. The cleaning of the sample, the ozone treatment and the sputtering itself take considerable amounts of time. All things considered, the procedure can take up to 4 hours for one prepared sample. It would be beneficial to have a setup that just has to be coated with the battery electrode and is ready to go.
A second drawback is the sample size. The sample size is limited by the size of the socket of the sputtering machine. This amounts to a maximum sample size of 2.5cm by 3.5cm. This limitation greatly reduces the variety of samples that can be used.
A third disadvantage of sputtering is the occurrence of so-called shadows on the sample. Shadows arise when the source material is deposited beyond the boundaries of the mask. This is because the substrate and the mask do not perfectly lie on top of each other and source material finds its way under the mask, onto the substrate. The risk is that shadows bleed over in each other and cause unwanted electrical connections. A possible solution for this problem is using an acrylic mask. It is more rigid and this makes it easier to fix its flat surface to the glass substrate.
A final problem is the probes chemical resistance. When cleaning the substrate with acetone to get rid of the electrode coating, the sputtered probes wash away as well with little resistance.

Using metal printing, the sample preparation time can be significantly decreased. Also, samples of many different sizes and dimensions can be used. The drawback of this method was that the metal printer could not reach the desired resolution. The lines and pads bleed over in each other rendering this method unusable.

6.1.2. PCB & Enclosure

The PCB and holder made in the PXL Makerspace with the laser cutter and PCB mill are a cost-effective way of developing this setup.

One difficulty was getting the pogo pins to line up evenly during soldering. There was a certain tolerance that had to be considered.

Another problem arose when clamping the PCB, holder and substrate together. The pogos have a relatively high spring force: 45 grams of preload and 108 grams of rated force [33]. When using 48 of these pogos, the force needed to compress increases greatly. This force made it very easy to damage the fragile gold probes on the glass substrate (see Figure 6.1). When damaged, the pogo pins would cease to make contact with the gold probes of the substrate and render the probe unusable.

In Figure 6.2, all the different components of the pogo probe can be seen. Figure 6.3 shows the complete enclosure with the PCB and pressure sensor.

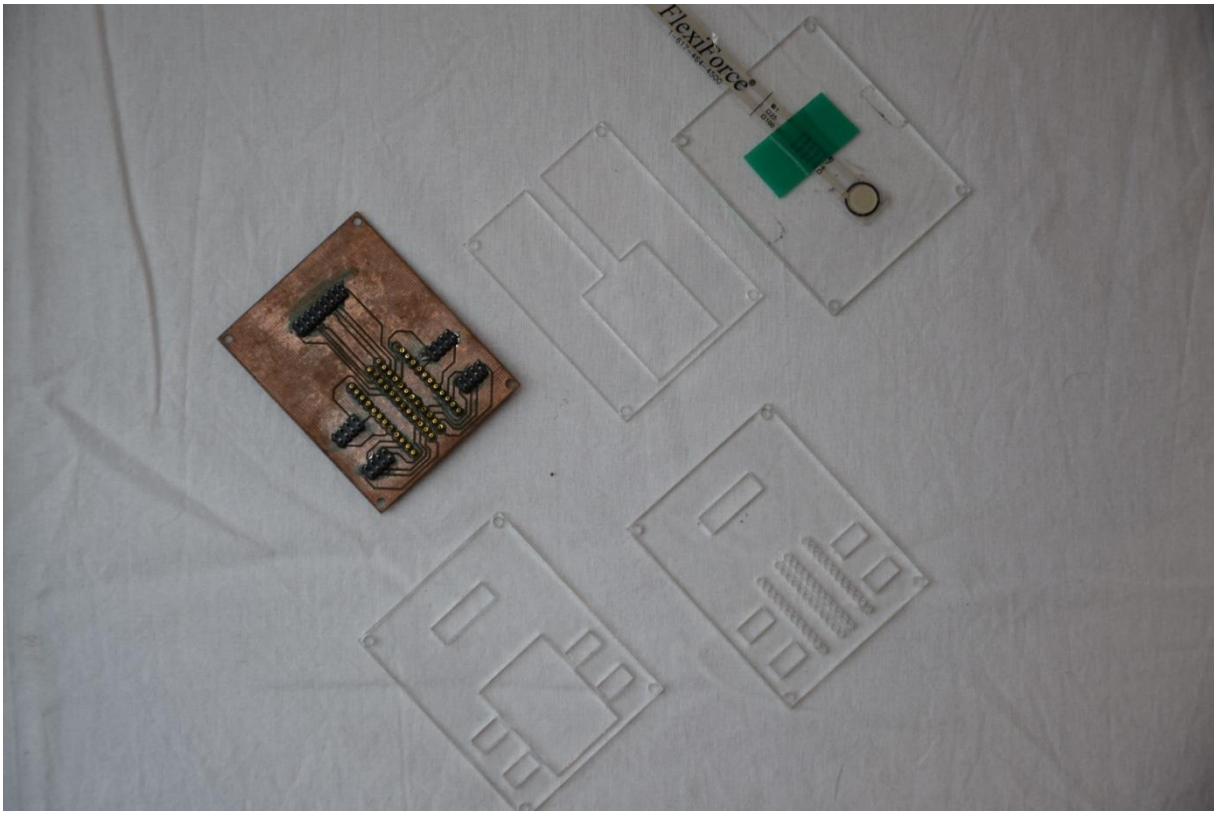

Figure 6.2: Components of the pogo pin probe

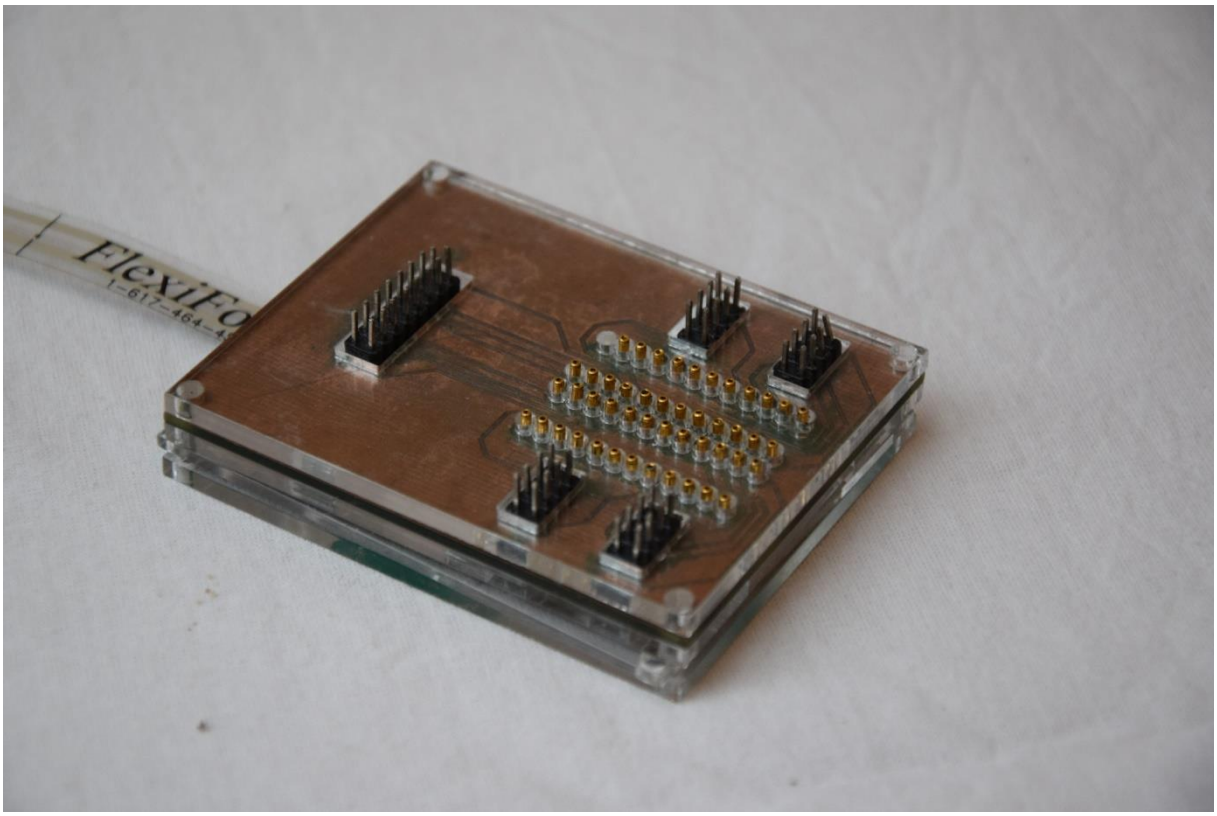

Figure 6.3: Pogo probe setup

6.1.3. Measurement Results

The first test was comparing the sheet resistance measurement of the Ossila 4PP to that of the new setup using a sample with a sputtered probe pattern. The sample had several problems. First, the probe pattern suffered from significant shadows. Second, the coating on the sample was uneven and not uniform and did not coat the entire pattern.

Using the Ossila 4PP with the probes centred in the middle of the sample (as prescribed in its manual [58]) we get a reference value for the sheet resistance. Two measurements were conducted at different output target currents (0.5mA and 1mA respectively). Each measurement samples ten values. Before each sample recording, the output current is incremented until the desired output current is reached.

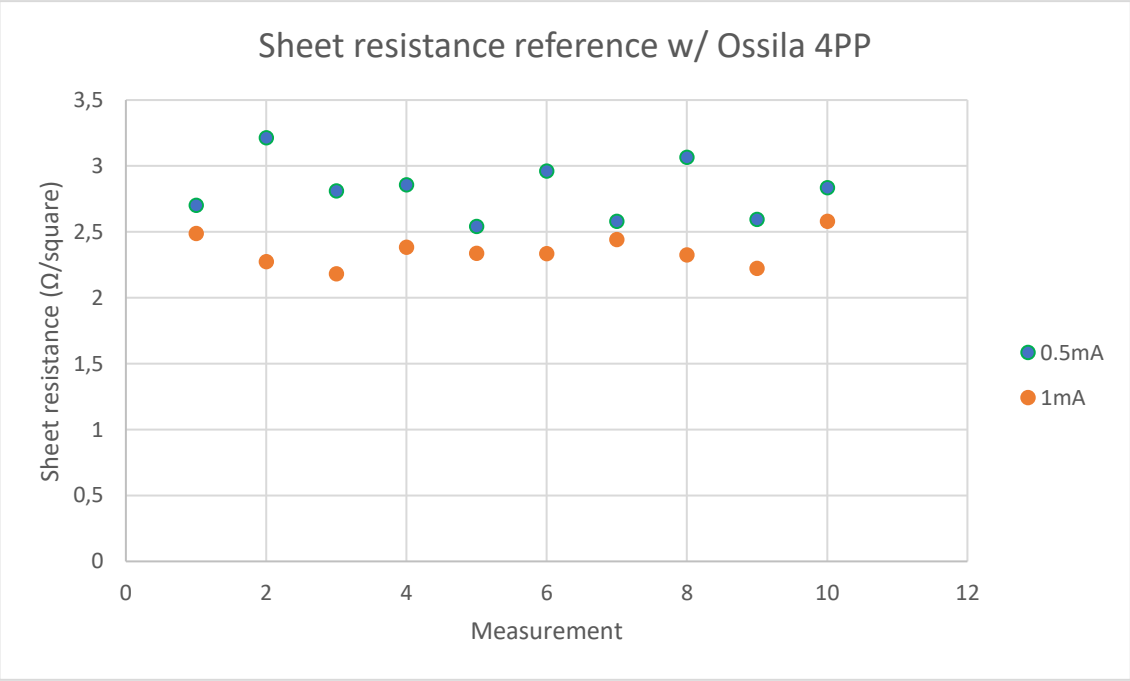

Figure 6.4: Sheet resistance as measured with the Ossila 4PP. Shows the resistance at the two different target currents

Table 1: Averages and Standard Deviations of sheet resistance measurement with 4PP

Ossila 4PP	0.5mA	1mA	TOTAL
AVG (Ω/square)	2.8172318	2.3578740	2.5875529
ST DEV	0.2088291	0.1148355	

The reference measurement gives us an average sheet resistance of 2,588 Ω/square, as can be observed in

Table 1. The standard deviations indicate the values are normally distributed and there is little variation from the mean.

Next, we see the sheet resistance measured of a certain area of the substrate with the new setup, using the measuring setup illustrated in chapter 5.4. The output currents are 1mA and 2mA.

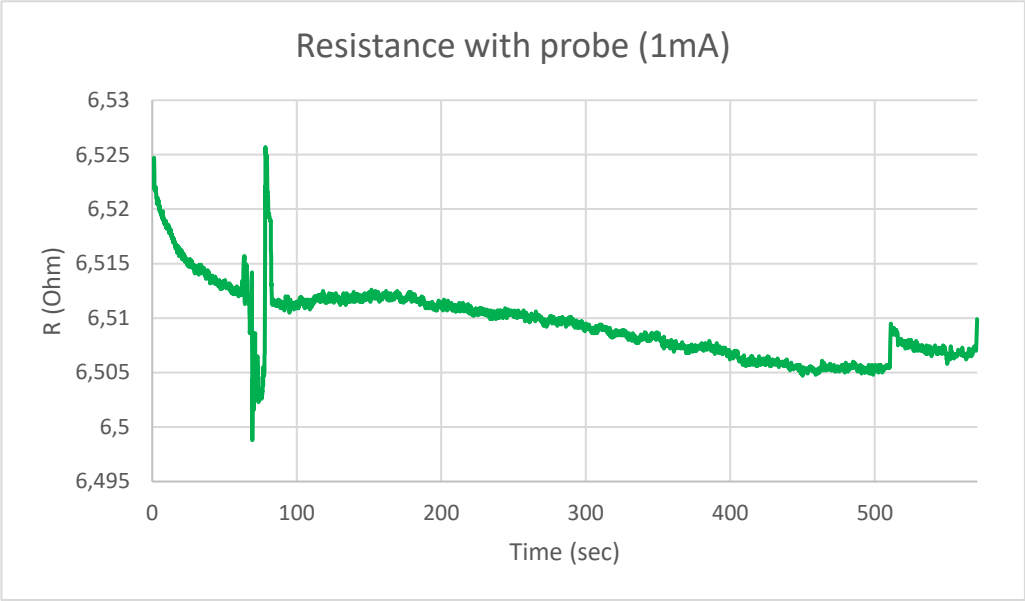

Figure 6.5: Sheet resistance with pogo pin probe at 1mA output current

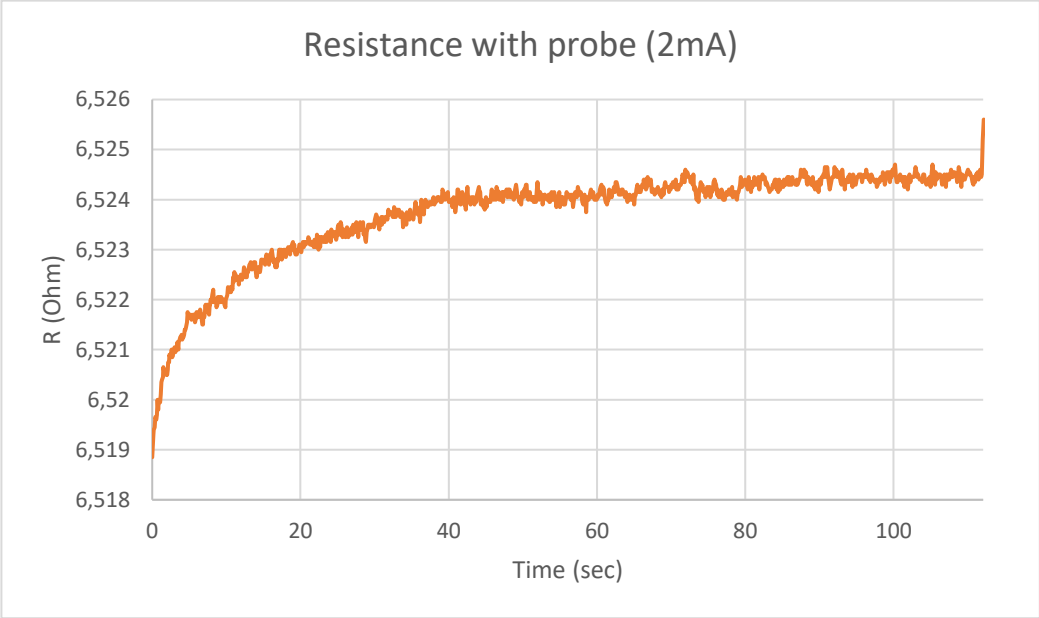

Figure 6.6: Sheet resistance with pogo pin probe at 2mA output current

Table 2: Averages and Standard Deviations of probe measurements at 1mA and 2mA input current

Probe	1mA	2mA	TOTAL
AVG (Ω)	6.5102215	6.5236550	6.5169382
ST DEV	0.0036272	0.0009928	

As can be seen in Table 2, the resistance measured with the pogo pin probe setup is 6.517Ω. The standard deviation again indicates little variation from the mean. When applying a larger current, the voltage across two probes increases and the calculated resistance stays the same, as can be seen when comparing Figure 6.5 and Figure 6.6.

When comparing the Ossila 4PP to the self-made setup, the results from the 4PP are denoted as being Ω/square. This is simply an alternative, but dimensionally equal, unit to Ω. It is used to prevent misinterpretations as a measurement in Ohms does not differentiate between surface or bulk resistance. A measurement denoted as Ω/square simply specifies that what is talked about is surface resistance. There is no misinterpretation [59] [60].

When comparing the two average values of the two different measurement setups, it is clear that they are not equal. This can be due to the fact that the area of the electrode coating that was measured was different in both cases. Due to the spatial resistance differences that can occur, the measured resistance was not equal.
Also considered was that there was extra resistance added in the Pogo Pin Probe from the pogo pins and copper traces of the PCB. This was not likely a problem as the resistance of the pogos used is less than 30mΩ [33] and the resistance of copper amounts to 350.0174μΩ m [61]. All extra resistances considered, this would not significantly impact the result of the measurement.

The Pogo Pin Probe is a positive development. It is an easy measuring tool, but the sample preparation time and the fragility of the sample make it that this method is not considered as a viable setup for the problem at hand.

6.2. Setup 2: 3D Printed Probe

Next up, the results obtained with the mask used in the 3D printed probe are presented. Afterwards, the 3D prints themselves are discussed, followed by the results of the ink tests and the screen printing.

6.2.1. Mask

Making a mask with the desired line resolution was possible using the laser cutter present and the PXL Makerspace. This is good news as it is an easy production process and cost effective.
A drawback of using a thin aluminium sheet is its strength. Great caution has to be taken when handling such a mask. The micro lines of the mask are prone to breaking. This also hinders good application of the ink when screen printing (see 6.2.4).

6.2.2. 3D Print

Figure 6.7: Dektak Profilometer [69]

Using the Original Prusa SL1 3D printer, good results were obtained (see Figure 6.10 and Figure 6.11), both in the resolution of the line width as in the depth of the channels. This can be seen when looking at Figure 6.9, where the relief of the substrate is measured using a Dektak Profilometer. A profilometer is used to get an idea of the topography of an object by scanning a line with a stylus across the surface [62]. A profilometer can have various sensors to detect the vertical movement of the stylus. These sensors include linear variable differential transformers (using coils and a ferromagnetic core that influence a voltage [63]), three plate capacitive sensors (objects effect the electrical field created by the sensor [64]) and optical levers (using a laser light reflecting of a mirror [65]).

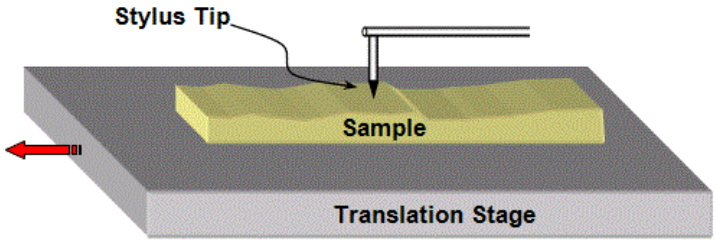

Figure 6.8: Diagram of stylus tip of a profilometer contacting a sample [65]

One flaw arose when heat treating the substrate to cure the coated ink with near infrared light. Occasionally, after multiple light pulses in short concession, the substrate would show a slight bend. This can be attributed to the fact that the platform on which the substrate is placed is smaller than the substrate itself. In combination with the high temperature from the light, the substrate would bend due to its own weight. This might impact the contact between the top and bottom probe.

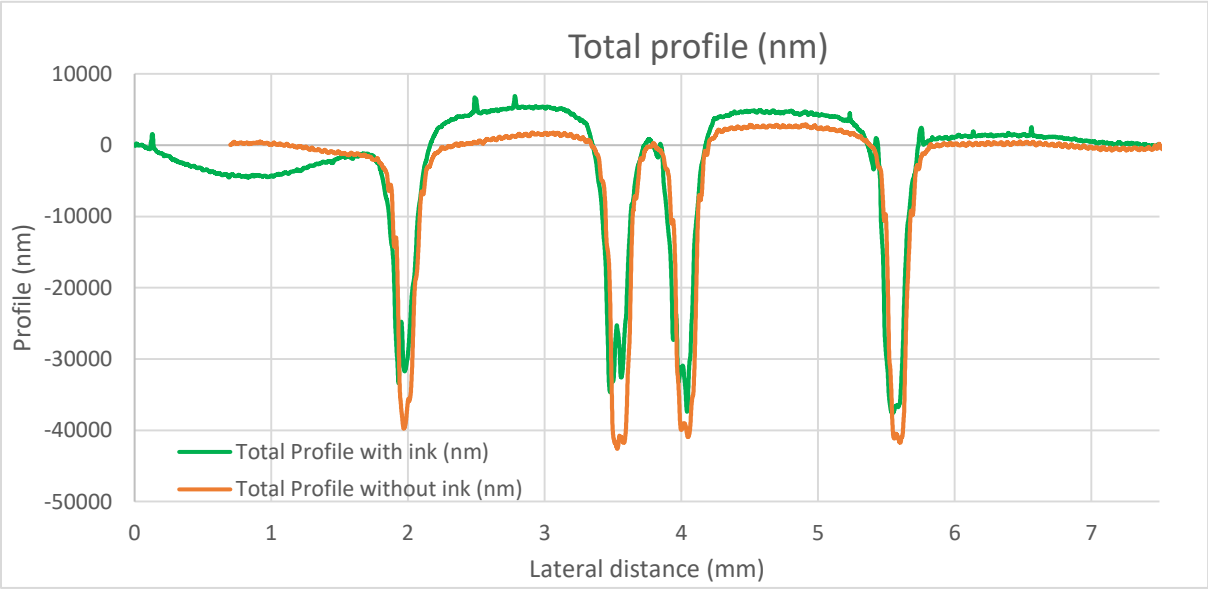

Figure 6.9: Profilometer plots of the 3D substrate, before and after the deposition of the conductive ink

Figure 6.10: Bottom probe 3D printed substrate

Figure 6.11: Top probe 3D printed substrate

6.2.3. Ink Coating

The four inks described in the previous section were coated on a resin printed substrate and tested on the criteria mentioned in 5.2.4.1.

The first three criteria (layer thickness, particle size and electrical resistance) can all be determined from the datasheet of the inks. Thus, the four inks tested were all preselected with these criteria in mind and consequently passed these first three criteria.

The curing cycle worked for every ink and made sure the ink became one solid, conductive layer. After curing, the inks were tested on their adhesion to the substrate. All inks were relatively sturdy, but it should not come as a surprise that with enough force, all inks could be chipped or scraped of the surface of the substrate.
When subjecting the inks to the chemical resistance test, one ink showed significantly better results. As can be seen in Figure 6.12, only the Loctite ECI 1011 E&C ink could resist a wash with both acetone and ethanol. Considering these results (and in particular the chemical resistance test), the *Loctite ECI 1011 E&C* was selected to use as the screen printing ink.

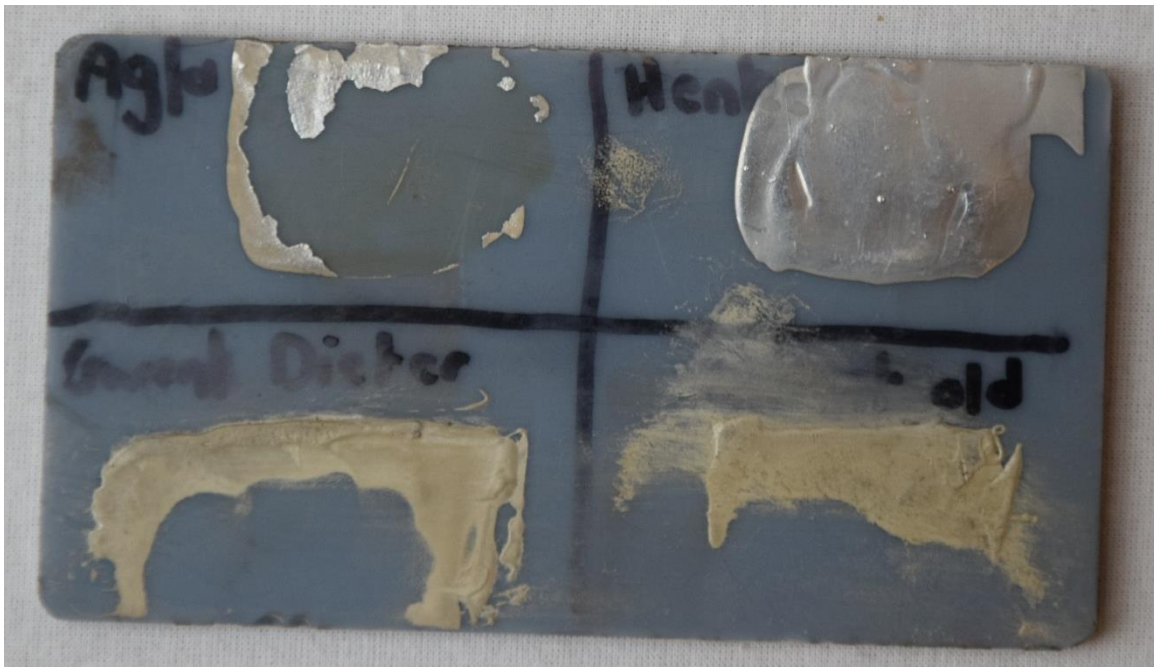

Figure 6.12: Results after ink tests. Top left: AGFA Orgacon Ink, top right: Loctite ECI , bottom left: Gwent C2131014D3, bottom right: Gwent C2090210D12 .

6.2.4. Screen Printing

After the mask and 3D print were completed and an suitable ink selected, screen printing could be done. As can be seen in Figure 6.13, this did not yield a good result. The force of the squeegee, together with the fragile nature of the mask, caused the mask to be destroyed.

After cleaning the substrate and curing the ink, it can be observed that the ink does settle in the micro lines (as seen in Figure 6.14) and forms an electric connection. With the use of a stronger mask material, e.g. inox or steel, or with an expensive mesh screen that can reach the desired resolution, the screen printing could yield better results.

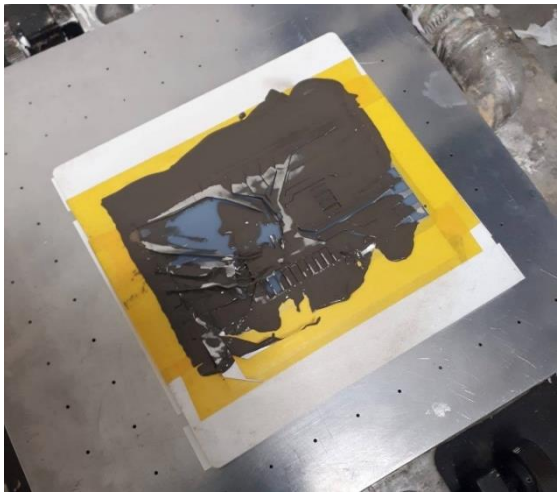

Figure 6.13: Substrate and mask after passing of squeegee

Figure 6.14: 3D printed substrate after screen printing and cleaning

6.2.5. Measurement Results

Because of the failure to provide a probe with the techniques described in the previous sections, no measurement results could be obtained for this setup.

Even though no measurement results were obtained, this setup shows potential. If a decent mask can be acquired that can create a fine pattern, a sturdy probe with good surface topology could be created.

6.3. Setup 3: PCB Probe

6.3.1. Printed Circuit Board

The manufactured PCBs are of good quality (Figure 6.17)

To check the profile of the micro 4-line probe, the Dektak Profilometer was used. From Figure 6.15 and Figure 6.16, the four (copper) traces are clearly visible. They protrude slightly from the surface, which is favourable because this can improve the contact between the top and bottom probe lines. A downside of the PCB are the deep gaps between the lines. When coating the PCB, these gaps do not fill and prevent an even coat (Figure 6.16). In turn, this uneven coat can influence the conductance measurement.

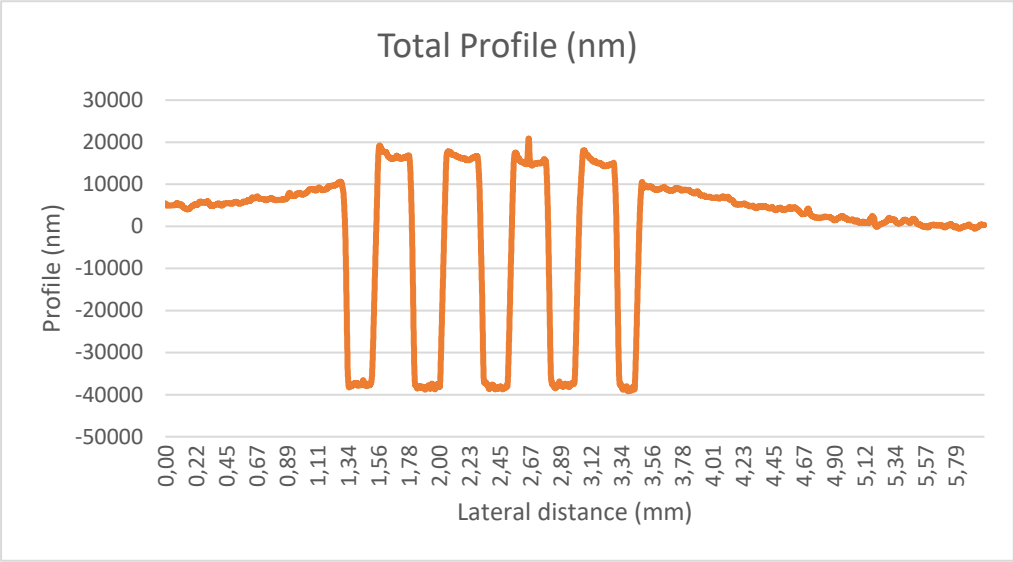

Figure 6.15: Profile plot of PCB micro lines before coating

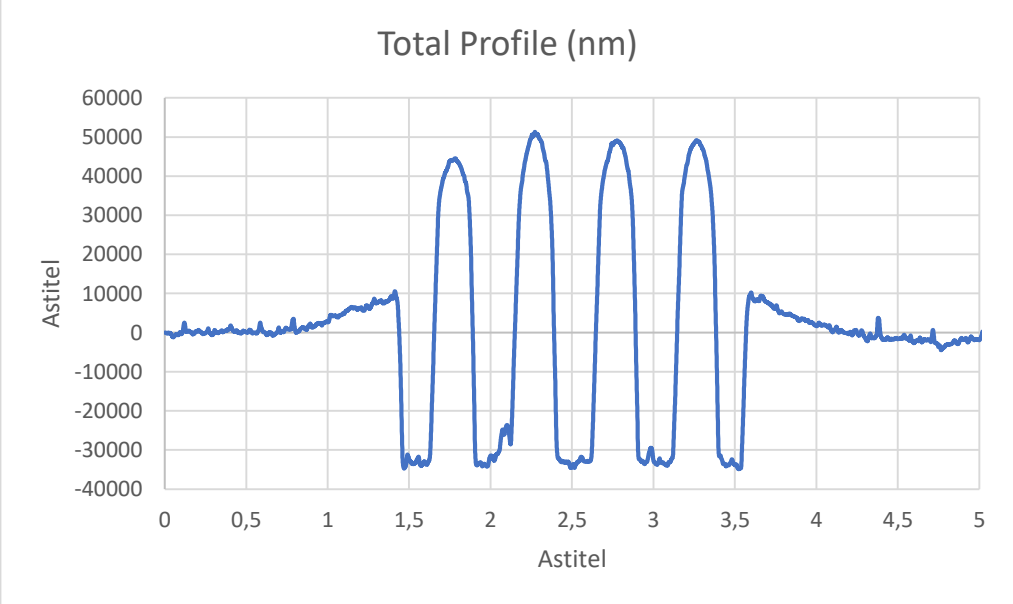

Figure 6.16: Profile plot of PCB micro lines after coating

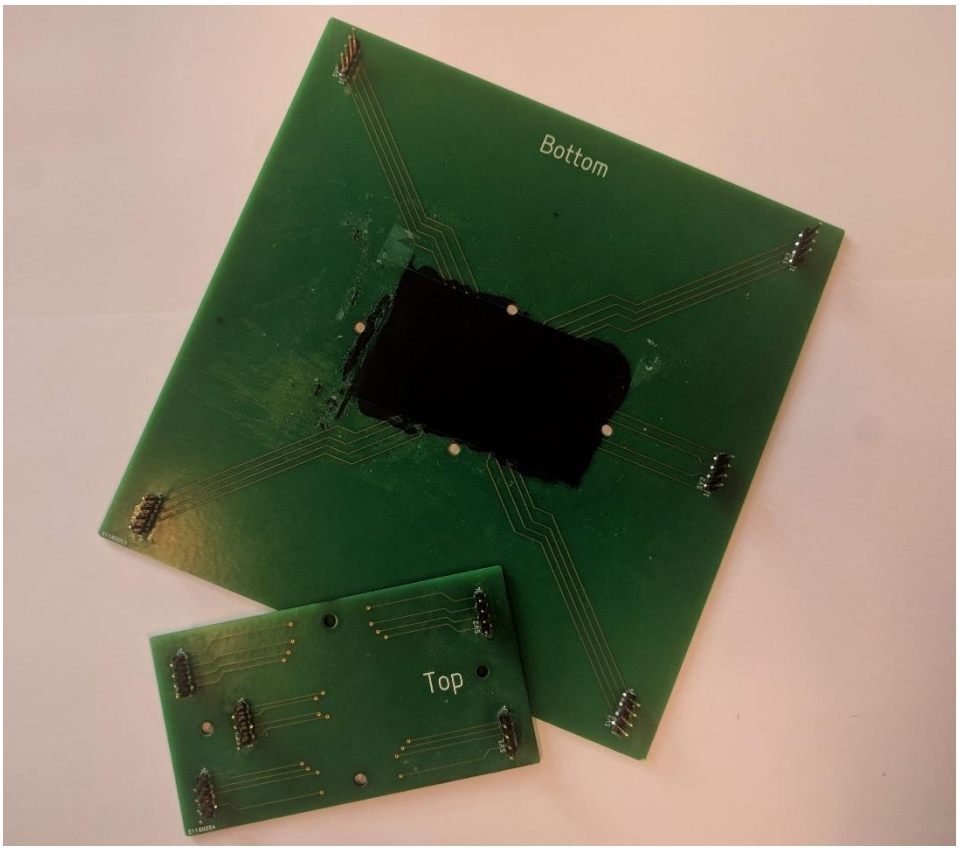

Figure 6.17: Top and Bottom PCB

6.3.2. Measurement Results

First, the sheet resistance was measured using the new PCB probe setup. After, these results were compared to the result obtained from the Ossila Four Point Probe device. For this measurement, only the bottom PCB was used.

Next, the full setup is used to gather bulk resistance measurements. For this, the two PCBs were placed on top of each other. The two electrode leads of the Keysight measuring unit to the outer lines of a four-line probe on one PCB. The other two leads are connected to the inner lines of the probe on the other PCB.

For each of the five regions of the probe, a series of measurements was done. Each series is characterized by a different supply current (0.05mA, 0.5mA, 5mA and 50mA). Every series lasts for 20 seconds and a data point is captured at a 10Hz frequency.

6.3.2.1. Sheet resistance

In each figure from Figure 6.18: Sheet Resistance Top Left Probe to Figure 6.22: Sheet resistance of Bottom Right probe, the following trends can be seen:

For each applied current, the measured resistance is roughly the same for that specific area. Except when a current of 0.05mA was applied, the number would deviate and drop lower. There also is more noise, as can be seen when comparing the standard deviation of the measurements. This phenomenon can be explained due to the fact that 0.05mA is such a small current that it is also influenced by noise. The minimum source resolution of the Keysight device is 1pA and the minimum measurement resolution is 100nV [55]. From those resolution values it can be concluded that the noise is not due to the measuring device used. Instead it could be attributed to noise caused in the electrode leads and connections with the PCB. This makes the resistance calculation differ from the rest of the measurements.

Following next are the resistance plots of each region of the probe and the tables containing the average resistance values and the standard deviation of each plot.

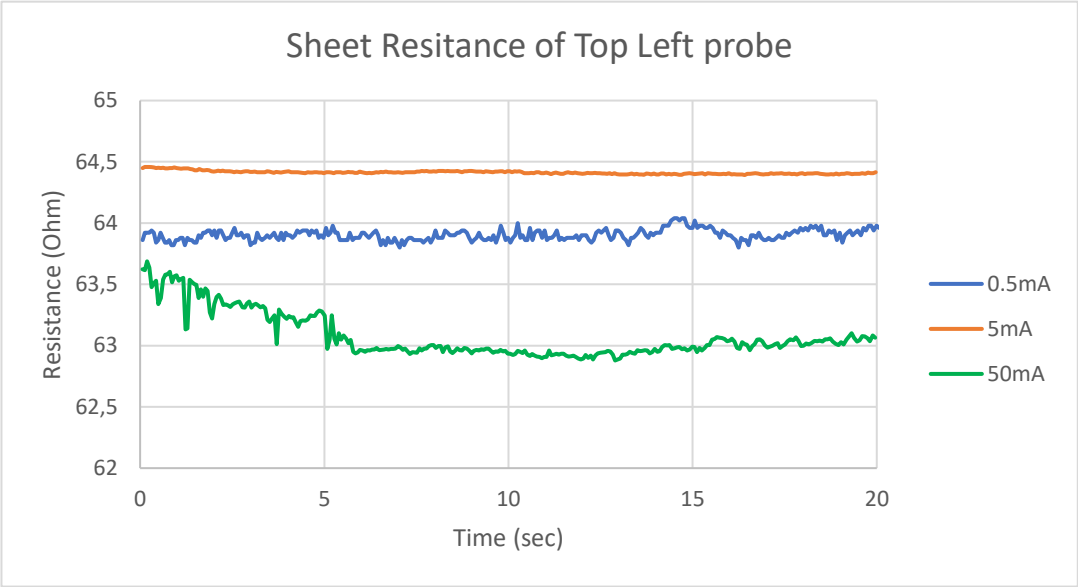

Figure 6.18: Sheet Resistance Top Left Probe

Table 3: Standard Deviations and Averages of Top Left region

Top Left	0.5mA	5mA	50mA	TOTAL
AVG (Ohm)	63.90243	64.41365	63.0808	63.79896
ST DEV	0.044744	0.013741	0.187832	

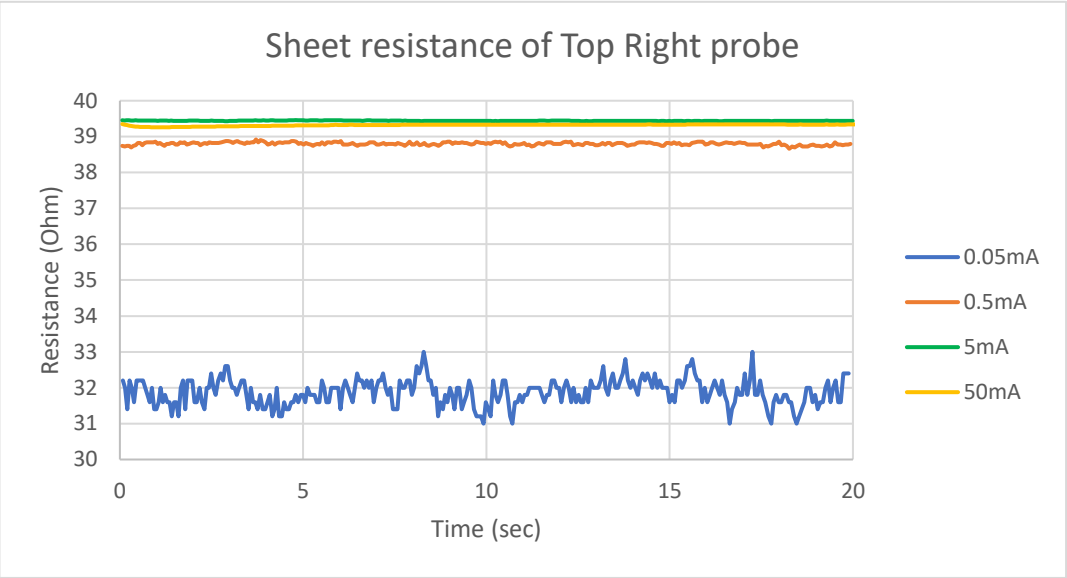

Figure 6.19: Sheet Resistance of Top Right probe

Table 4: Standard Deviations and Averages of Top Right region

Top Right	0.05mA	0.5mA	5mA	50mA	TOT CORRECTED
AVG (Ohm)	31.87442	38.80219	39.44147	39.31988	39.18785
ST DEV	0.364236	0.040288	0.006361	0.022743	

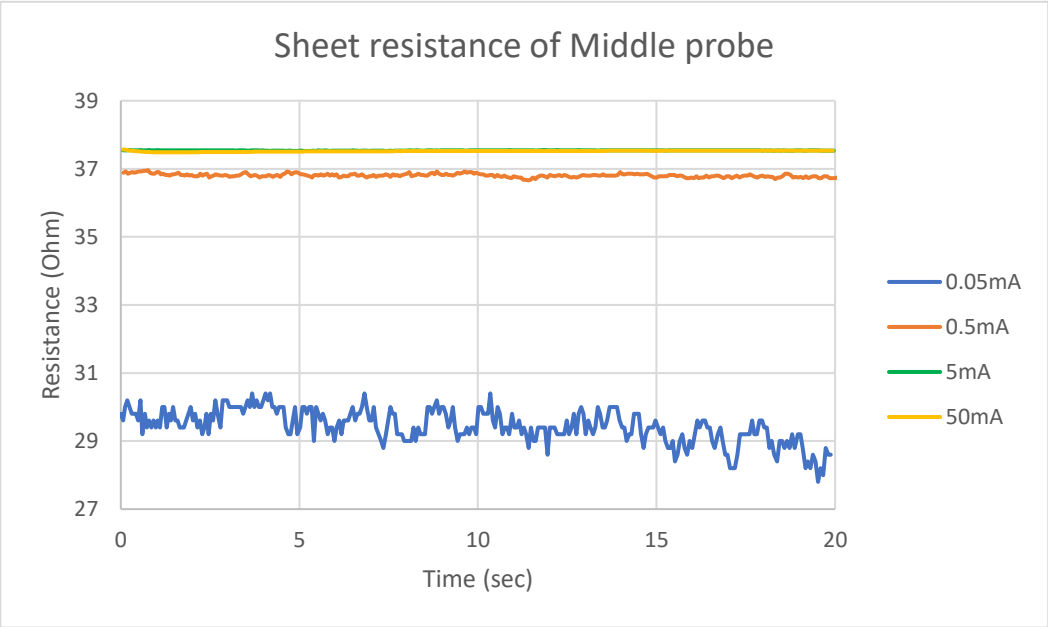

Figure 6.20: Sheet Resistance of Middle probe

Table 5: Standard Deviations and Averages of Middle region

Middle	0.05mA	0.5mA	5mA	50mA	TOT CORRECTED
AVG (Ohm)	29.448	36.806	37.839	37.518	37.288
ST DEV	0.4818	0.0518	0.0054	0.0142	

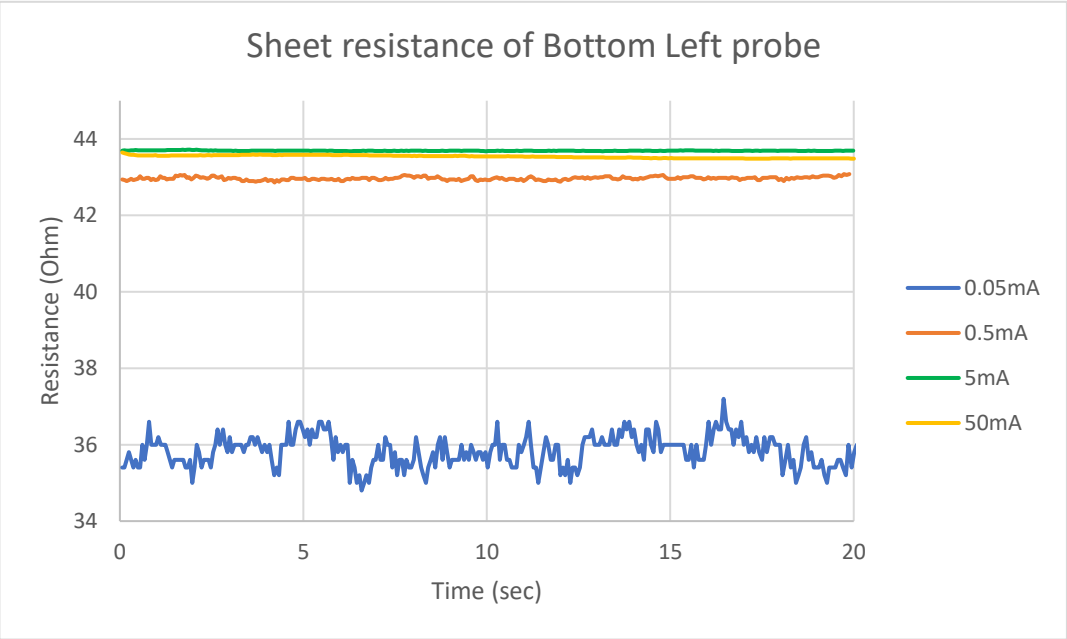

Figure 6.21: Sheet Resistance of Bottom Left probe

Table 6: Standard Deviations and Averages of Bottom Left region

Bottom Left	0.05mA	0.5mA	5mA	50mA	TOT CORRECTED
AVG (Ohm)	35.827	42.968	43.692	43.54	43.4
ST DEV	0.4024	0.0409	0.007	0.0362	

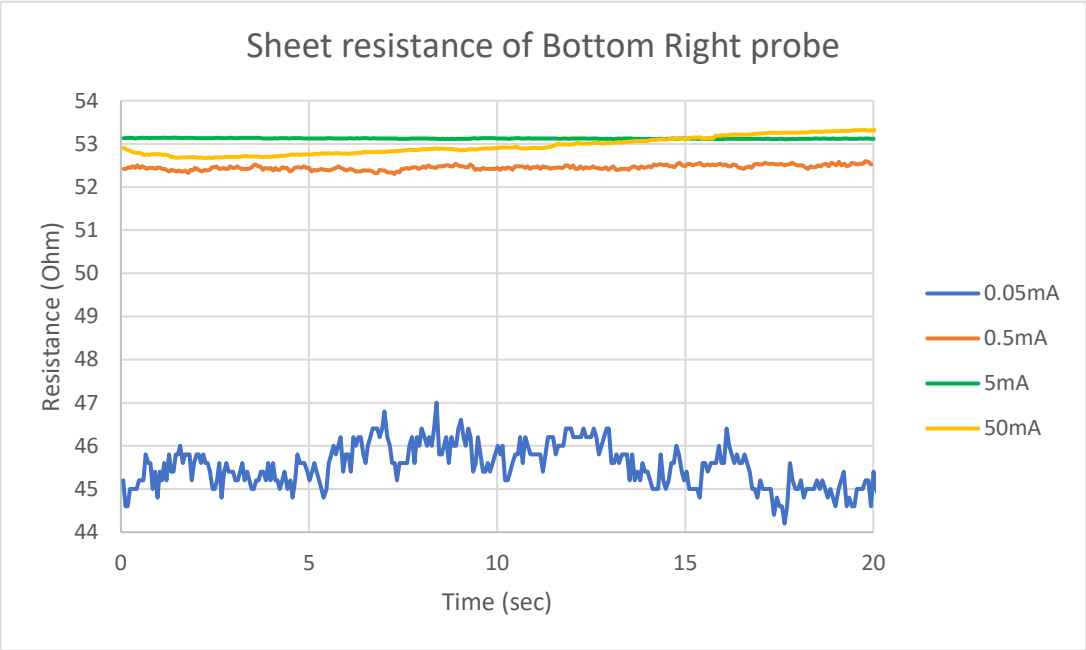

Figure 6.22: Sheet resistance of Bottom Right probe

Table 7: Standard Deviations and Averages of Bottom Right region

Bottom Right	0.05mA	0.5mA	5mA	50mA	TOT CORRECTED
AVG (Ohm)	45.519	52.452	53.124	52.942	52.84
ST DEV	0.505	0.0544	0.0083	0.2014	

When comparing the average sheet resistances of each region, it can be observed that they do not have the same value. The regional resistance differences can clearly be distinguished. This phenomenon can be attributed to the fact that the coating procedure of the electrode onto the probe can never be perfect. There are also defects in the coating itself. Some parts of the coating might contain more conductive carbon particles than others. This happens when the coating is not properly mixed. Likewise, different amounts of solvent could have evaporated, furthermore changing the physical properties of the coating form region to region. This setup can be a useful tool to detect these differences, certainly when increasing the number of lines on the PCB. This can be by either adding more 4-line probes on the same sized area or increase the area size.

To see if the sheet resistance measured with the PCB probe would be comparable to other methods, the Van Der Pauw method was used, as the Ossila 4PP could not measure a substrate with the size of the PCB. The Van Der Pauw method also used four point-probes like a linear four-point probe, but the probes using the Van Der Pauw method are placed on the edges of the sample. This allows the method to provide the resistivity of a whole sample of arbitrary size and shape.
The resistance of the sample using the Van Der Pauw method came out to be 450Ω/square. This value is, evidently, not the same compared to that measured with the PCB probe. A possible reason for this inequality can be found when looking at the sample condition that have to be satisfied to get appropriate results. One of the conditions is that the sample has to be flat and have a uniform

thickness. Because of the nature of the PCB probe (with its four-lines that make the surface uneven), this condition is not met and could be the reason that the measured values of the two probes do not compare.

6.3.2.2. Bulk resistance

Next, the measurement results of the bulk resistance can be seen in Figure 6.23: Resistance measured at multiple probe locations at different input currents (0.05mA and 0,5mA) and different applied pressure to probes and Figure 6.24: Highlight of bulk resistance measurement. As can be observed, the measurements do not give conclusive results. When the two PCB probes are simply tightened together, the read out values show negative resistance values of around -10Ω. That is because the voltage measured by the Keysight unit is negative. This negative value is a standard value coming from the measuring unit when there is no voltage detected. The error also does not lie at the applied input current, as multiple currents were set (0.05mA, 0.5mA and 5mA), which did not change the output voltage. A probable cause for this error would be that the top probe does not contact the coating on the bottom probe. This presumption was confirmed when pressing down on the top probe. The resistance values spiked and showed positive and plausible values. This can clearly be seen in Figure 6.23: Resistance measured at multiple probe locations at different input

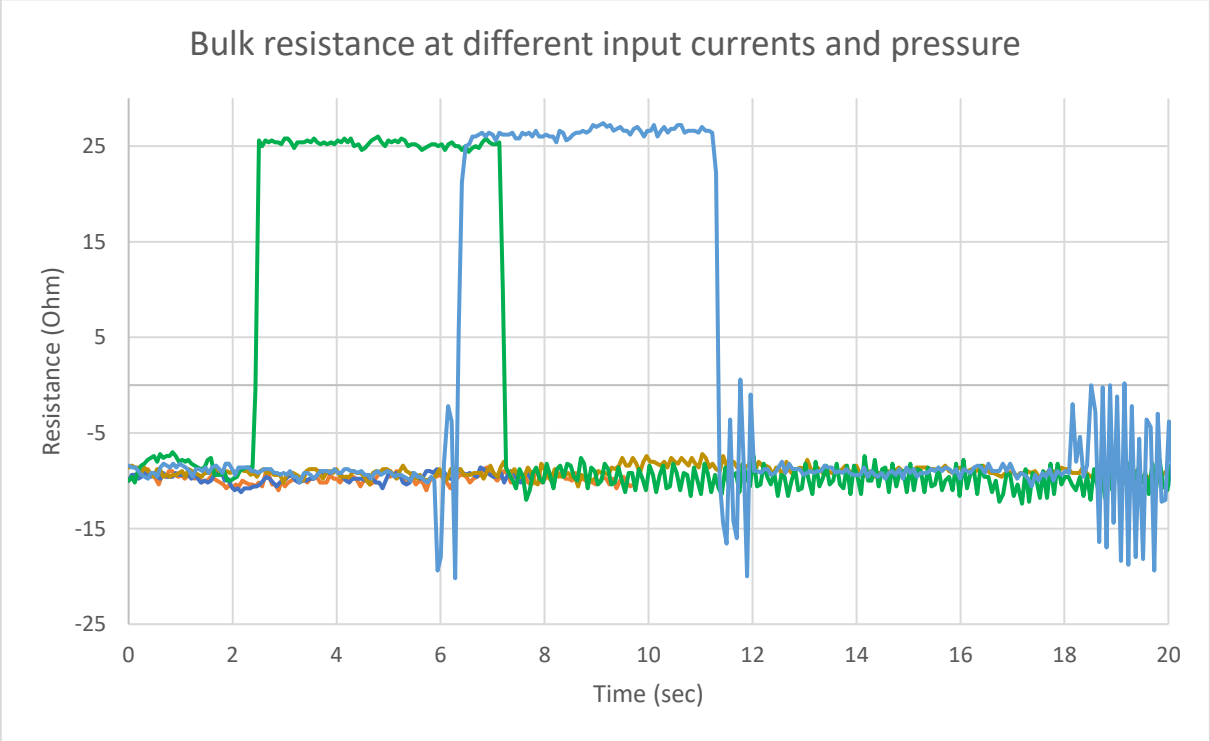

Figure 6.23: Resistance measured at multiple probe locations at different input currents (0.05mA and 0,5mA) and different applied pressure to probes

currents (0.05mA and 0,5mA) and different applied pressure to probes, where the *green* and *blue* graphs show this spike after the top probe is pressed down onto the bottom probe. In this case, the average resistance comes out to 25.28Ω (*green*) and 26.42Ω (*blue*), respectively.

In Figure 6.24, the *blue* graph of Figure 6.23 is magnified. Here, multiple spikes can be observed. They all correspond to a time where the probes are pressed onto each other. At 25 seconds the input current was increased to 0.5mA. The measured resistance does not change, which is what is expected and wanted.

Figure 6.24: Highlight of bulk resistance measurement

What can be deduced from this is that the probe a good method to determine regional differences in a battery electrode coating. For surface resistivity measurements, it could not be confirmed that the measured values were correct. Additional testing has to be done, including developing a PCB Probe with a flatter surface in order to get a more uniform electrode coating.

7. Conclusion

Of the three setups developed, the PCB probe showed the most promising results. While the Pogo Pin Probe had problems with the sample (it was prone to damage and not reusable) and the 3D Printed Probe was never fully realized because of the frail aluminium mask, the PCB Probe was both easy to produce and easy to re(use).Thanks to the repetition of the line probe, spatial differences in a battery electrode coating can be compared using the measured sheet resistance. Comparison to an existing setup was challenging as the sample was too big for the 4PP and did not meet the requirements for a decent Van Der Pauw measurement. Due to these limitations, it was difficult to compare the measurement results of the PCB Probe to those of existing setups.

This probe is a viable option to measure the bulk resistivity of a battery electrode, provided that there is good contact between the top and bottom probe. More testing also has to be done to confirm that these results are comparable to existing setups.

It can be concluded that the developed setup can mostly be used to get an idea of the spatial/regional resistance differences in a solid battery electrode.

Future improvements that can be made mostly have to do with the probe's topology. The four-line probe can be shrank down to true micrometre scale as in [20]. This way, more lines can fit on the PCB and the spatial differences can be examined in much more detail. An important improvement would be the topography of the lines. Elimination of the gaps between the lines as seen in Figure 6.15 would improve the integrity of the battery electrode. The less destructive the probe is the better. It could yield more realistic measurement results.

References

[1] FOUR-POINT-PROBES, “Understanding Volume Resistivity Measurements,” Bridge Technology, 2017. [Online]. Available: http://four-point-probes.com/understanding-volume-resistivity-measurements/. [Accessed 23 03 2019].

[2] L. Critchley, “Editoral Feature: How Thin Film Batteries Work,” Azo Materials, 7 05 2018. [Online]. Available: https://www.azom.com/article.aspx?ArticleID=15815. [Accessed 26 02 2019].

[3] Samsung SDI, “Technology: The Four Components of a Li-ion Battery,” Samsung SDI, 2016. [Online]. Available: https://www.samsungsdi.com/column/technology/detail/55272.html. [Accessed 26 02 2019].

[4] Battery University, “What is the Function of the Separator?,” Isidor Buchmann, 08 01 2019. [Online]. Available: https://batteryuniversity.com/learn/article/bu_306_battery_separators. [Accessed 07 25 2019].

[5] Wikipedia, “Thin film lithium-ion battery,” Wikimedia Foundation, Inc., 12 02 2019. [Online]. Available: https://en.wikipedia.org/wiki/Thin_film_lithium-ion_battery. [Accessed 07 18 2019].

[6] MTI Corp, “Large Automatic Film Coater with 12"W x 24"L Vacuum Chuck - MSK-AFA-II-VC,” MTI Corp, 17 06 2017. [Online]. Available: https://www.youtube.com/watch?v=8E47M9Ze66w. [Accessed 14 08 2019].

[7] S.-H. P. P. J. K. G. C. J. C. V. N. &. J. N. C. Ruiyuan Tian, “Quantifying the factors limiting rate performance in battery electrodes,” *Nature Communications,* vol. 10, 2019.

[8] S. Hymel, “Measuring Internal Resistance of Batteries,” SparkFun Electronics, [Online]. Available: https://learn.sparkfun.com/tutorials/measuring-internal-resistance-of-batteries/internal-resistance. [Accessed 10 08 2019].

[9] Battery University, “How does Rising Internal Resistance affect Performance?,” Cadex Electronics Inc., 10 07 2019. [Online]. Available: https://batteryuniversity.com/learn/article/rising_internal_resistance. [Accessed 10 08 2019].

[10] Energizer Holdings Inc. , “Battery Internal Resistance,” *Energizer Technical Bulletin,* pp. 1-2, 12 2005.

[11] E. Amato, “Battery Conductance & How to Apply It,” Franklin Electric, 27 05 2019. [Online]. Available: https://franklingrid.com/landing/blog/battery-conductance/. [Accessed 10 08 2019].

[12] Midtronics, “Battery Conductance: Stationary Power Battery Management - Questions & Answers,” [Online]. Available:

http://www.midtronics.com/component/simpledownload/?task=download&fileid=images%2Fstories%2Fpdf%2F190-055A_QA.pdf. [Accessed 17 04 2019].

[13] Virtual Amrita Laboratories Universalizing Education, “Resistivity by Four Probe Method,” Amrita Vishwa Vidyapeetham University, 2019. [Online]. Available: http://vlab.amrita.edu/?sub=1&brch=282&sim=1512&cnt=1. [Accessed 27 02 2019].

[14] Ossila Ltd, “Sheet Resistance: A Guide to Theory,” Ossila Ltd, [Online]. Available: https://www.ossila.com/pages/sheet-resistance-theory. [Accessed 05 03 2019].

[15] FOUR-POINT-PROBES, “Four-Point Probe Manual,” Bridge Technology, 2017. [Online]. Available: http://four-point-probes.com/four-point-probe-manual/. [Accessed 27 02 2019].

[16] Haldor Topsøe Semiconductor Devision, “Geometric Factors in four point probe resisitivity measurement,” *The Bulletin,* 05 05 1966.

[17] S. W. Peterson and W. R. Dean, “Direct Measurements of Effective Electronic Transport in Porous,” *Journal of The Electrochemical Society,* vol. 161, no. 14, pp. A2175-A2181, 16 10 2014.

[18] T. C. T. S. T. O. M. L. P.-J. B. G. P. N. H. B. T. G. G. a. W. V. Nils Mainusch, “New Contact Probe and Method to Measure Electrical,” *Energy Technology,* no. 4, p. 1550 – 1557, 2016.

[19] M. B. Heaney, “Electrical Conductivity and Resistivity,” in *Electrical Measurement, Signal Processing, and Displays*, CRC Press LLC, 2004, pp. 7.1 - 7.14.

[20] A. A. R. N. S. G. J. D. F. A. D. C. J. E. V. D. R. W. a. B. A. M. Bryson J. Lanterman, “Micro-Four-Line Probe to Measure Electronic Conductivity and Contact Resistance of Thin-Film Battery Electrodes,” *Journal of The Electrochemical Society,* vol. 162, no. 10, pp. 2145-2151, 2015.

[21] Van Loon Chemical Innovations BV, “Corrosion Testing via Electrochemical Impedance Spectroscopy (EIS),” Van Loon Chemical Innovations BV, 2018. [Online]. Available: https://vlci.biz/corrosion-testing-via-electrochemical-impedance-eis/. [Accessed 28 02 2019].

[22] Wikipedia, “Dielectric spectroscopy,” Wikimedia Foundation, Inc., 11 06 2019. [Online]. Available: https://en.wikipedia.org/wiki/Dielectric_spectroscopy. [Accessed 19 07 2019].

[23] Gamry, “Basics of Electrochemical Impedance Spectroscopy,” Gamry Instruments, 2019. [Online]. Available: https://www.gamry.com/application-notes/EIS/basics-of-electrochemical-impedance-spectroscopy/. [Accessed 23 07 2019].

[24] M. M. K. S. C. W. T. S.-G. D. S. D. Andrea, “Characterization of high-power lithium-ion batteries by electrochemical impedance spectroscopy. I. Experimental investigation,” *Journal of Power Sources,* vol. 196, p. 5334–5341, 2011.

[25] A. Lasia, “Electrochemical Impedance Spectroscopy and its Applications,” *Modern Aspects of Electrochemistry,* vol. 32, pp. 143-248, 1999.

[26] A. G. R. V. N. A. S. B. J.L. Yagüe, “A new four-point probe design to measure conductivity in polymeric thin films,” *Affinidad,* vol. LXX, no. 563, pp. 166-169, 2013.

[27] CADD Centre, “AutoCAD Mechanical,” [Online]. Available: https://www.caddcentre.com/autocad-mechanical-software-training.php. [Accessed 28 12 2019].

[28] M. Hughes, “What is PVD Coating,” Semicore Equipment, Inc., [Online]. Available: http://www.semicore.com/what-is-pvd-coating. [Accessed 28 12 2019].

[29] LNF Wiki, “Sputter deposition,” University of Michigan, 09 05 2019. [Online]. Available: http://lnf-wiki.eecs.umich.edu/wiki/Sputter_deposition. [Accessed 31 07 2019].

[30] N. Hardy, “Thin Film Deposition By Sputtering: Essential Basics,” Semicore Equipment, Inc., 07 10 2013. [Online]. Available: http://www.semicore.com/news/70-thin-film-deposition-sputtering. [Accessed 31 07 2019].

[31] Samco Inc., “The Basics of UV-Ozone Cleaning of Surfaces,” [Online]. Available: https://www.samcointl.com/basics-uv-ozone-cleaning-surfaces/. [Accessed 28 12 2019].

[32] P. Hart, “Using Pogo Pins to Add Electrical Connectivity to Your 3D Printed Fixtures,” Javelin Technologies Inc., 27 10 2016. [Online]. Available: https://www.javelin-tech.com/blog/2016/10/pogo-pins-3d-printed-fixtures/. [Accessed 1 08 2019].

[33] Smiths Interconnect Devices, Inc., *Technical Datasheet: Series SS & GSS, .100 Centers.*

[34] SparkFun Electronics, “FlexiForce Pressure Sensor - 1lb.,” SparkFun Electronics, 2017. [Online]. Available: https://www.sparkfun.com/products/8713. [Accessed 08 08 2019].

[35] Jimblom, “Voltage Dividers,” Sparkfun Electronics, 2013. [Online]. Available: https://learn.sparkfun.com/tutorials/voltage-dividers. [Accessed 08 08 2019].

[36] Jimblom, “Force Sensitive Resistor Hookup Guide,” Sparkfun Electronics, 2013. [Online]. Available: https://learn.sparkfun.com/tutorials/force-sensitive-resistor-hookup-guide. [Accessed 08 08 2019].

[37] Prusa Research, “Original Prusa SL1,” Prusa Research, 2019. [Online]. Available: https://www.prusa3d.com/original-prusa-sl1/. [Accessed 03 12 2019].

[38] Wikipedia, “Stereolithography,” Wikimedia Foundation, Inc., 10 11 2019. [Online]. Available: https://en.wikipedia.org/wiki/Stereolithography. [Accessed 3 12 2019].

[39] S. Frey, “Laser SLA vs DLP vs Masked SLA 3D Printing Technology,” The Ortho Cosmos, 23 03 2017. [Online]. Available: https://theorthocosmos.com/laser-sla-vs-dlp-vs-masked-sla-3d-printing-technology-compared/. [Accessed 03 12 2019].

[40] J. Průša, “Introducing Original Prusa SL1 – Open Source SLA 3D Printer by Josef Prusa,” Prusa Research, 22 09 2018. [Online]. Available: https://blog.prusaprinters.org/introducing-original-prusa-sl1-open-source-sla-3d-printer-by-josef-prusa/. [Accessed 03 12 2019].

[41] Prusa Research, “Grey Tough Resin 1kg,” Prusa Research, [Online]. Available: https://shop.prusa3d.com/en/resin/938-grey-tough-resin-1kg.html. [Accessed 08 12 2019].

[42] Prusa Polymers, *MATERIAL SAFETY DATA SHEET - Photopolymer Resin,* Praha: Prusa Research.

[43] Wikipedia, “Photopolymer,” Wikimedia Foundation, Inc., 06 11 2019. [Online]. Available: https://en.wikipedia.org/wiki/Photopolymer. [Accessed 08 12 2019].

[44] BASF SE, “Photoinitiators,” 2017. [Online]. Available: https://www.dispersions-pigments.basf.com/portal/basf/ien/dt.jsp?setCursor=1_556340. [Accessed 08 12 2012].

[45] Epoxy Technology Inc., “Tg - Glass Transition Temperature for Epoxies,” Billerica, MA, 2012.

[46] Agfa-Gevaert N.V., *Orgacon Product Information Sheet,* 2016.

[47] Henkel, *Loctite ECI 1011 E&C Technical Data Sheet,* 2016.

[48] RASA Industries, LTD., “Conductive paste from Gwent Electronic Materials (GEM),” RASA Industries, LTD., [Online]. Available: http://www.rasa.co.jp/business_prod/ncri_ramm/ramm_dev_center/polymer_paste/polymer_paste.html. [Accessed 05 12 2019].

[49] T. C. C. D. T. G. Eifion H. Jewell, “The development of printed electroluminescent lamps on paper,” *Journal of Print and Media Technology Research,* vol. I, no. 3, pp. 177-183, 2012.

[50] Wikipedia, “Screen printing,” Wikimedia Foundation, Inc., 23 11 2019. [Online]. Available: https://en.wikipedia.org/wiki/Screen_printing. [Accessed 04 12 2019].

[51] “Eagle Overview,” Autodesk Inc., 2019. [Online]. Available: https://www.autodesk.com/products/eagle/overview. [Accessed 10 12 2019].

[52] Wikipedia, “EAGLE (program),” Wikimedia Foundation, Inc., 02 12 2019. [Online]. Available: https://en.wikipedia.org/wiki/EAGLE_(program). [Accessed 10 12 2019].

[53] Eurocircuits, “SM – Soldermask,” [Online]. Available: https://www.eurocircuits.com/sm-solder-mask/. [Accessed 29 12 2019].

[54] Eurocircuits, “Who are we?,” 2018. [Online]. Available: https://www.eurocircuits.com/who-are-we/. [Accessed 03 01 2020].

[55] Keysight Technologies, “B2901A Precision Source/Measure Unit, 1 ch, 100 fA, 210 V, 3 A DC/10.5 A Pulse,” 2019. [Online]. Available: https://www.keysight.com/en/pd-1983568-pn-B2901A/precision-source-measure-unit-1-ch-100-fa-210-v-3-a-dc-105-a-pulse?cc=BE&lc=dut. [Accessed 11 12 2019].

[56] Wikipedia, “Four-terminal sensing,” Wikimedia Foundation, Inc., 13 07 2019. [Online]. Available: https://en.wikipedia.org/wiki/Four-terminal_sensing. [Accessed 11 12 2019].

[57] J. S. Mamaradlo, Informa USA, Inc., 30 06 2015. [Online]. Available: https://www.electronicdesign.com/blog/four-wire-sensing-can-make-or-break-your-measurements. [Accessed 11 12 2019].

[58] Ossila, “Four-Point Probe Measurement Guide,” [Online]. Available: https://www.ossila.com/pages/four-point-probe-measurement-guide?_pos=4&_sid=3c3c680fb&_ss=r. [Accessed 30 12 2019].

[59] G. Chase, “Ohms Per Square What!,” *ESD Journal,* pp. 1-3, 20 02 2008.

[60] Wikipedia, “Sheet resistance,” Wikimedia Foundation Inc., 18 12 2019. [Online]. Available: https://en.wikipedia.org/wiki/Sheet_resistance. [Accessed 30 12 2019].

[61] Engineering ToolBox, “Copper and Aluminum Wire - Electrical Resistance,” 2014. [Online]. Available: https://www.engineeringtoolbox.com/copper-aluminum-conductor-resistance-d_1877.html. [Accessed 08 01 2020].

[62] KNI Lab, “Dektak 3ST: Profilometer,” California Institute of Technology, 12 09 2019. [Online]. Available: https://lab.kni.caltech.edu/index.php/Dimension_Icon:_Atomic_Force_Microscope_(AFM). [Accessed 16 12 2019].

[63] Wikipedia, “Linear variable differential transformer,” Wikimedia Foundation Inc., 04 11 2019. [Online]. Available: https://en.wikipedia.org/wiki/Linear_variable_differential_transformer. [Accessed 31 12 2019].

[64] R. MacLachlan, “Capsense,” [Online]. Available: http://www.cs.cmu.edu/~ram/capsense/intro.html. [Accessed 31 12 2019].

[65] Australia Surface Metrology Lab, “Stylus Profilometry,” [Online]. Available: https://australiasurfacemetrologylab.org/new-page. [Accessed 31 12 2019].

[66] Wikipedia, “Four-terminal sensing,” Wikimedia Foundation, Inc., 13 07 2019. [Online]. Available: https://en.wikipedia.org/wiki/Four-terminal_sensing. [Accessed 13 08 2019].

[67] R. Kalmeijer, “mΩ-meter,” [Online]. Available: https://www.robkalmeijer.nl/techniek/electronica/electronicabladen/elektuur/1991/01/page44/index.html. [Accessed 13 08 2019].

[68] Structo Pte. Ltd., “Mask Stereolithography or MSLA,” [Online]. Available: https://www.structo3d.com/technology/. [Accessed 15 11 2019].

[69] National Institute of Standards and Technology, “NanoFab Tool: Bruker Dektak XT Profilometer,” [Online]. Available: https://www.nist.gov/laboratories/tools-instruments/nanofab-tool-bruker-dektak-xt-profilometer. [Accessed 31 12 2019].

[70] Keysight Technologies, “B2901A Precision Source/Measure Unit, 1 ch, 100 fA, 210 V, 3 A DC/10.5 A Pulse,” [Online].

Available: https://www.keysight.com/en/pd-1983568-pn-B2901A/precision-source-measure-unit-1-ch-100-fa-210-v-3-a-dc-105-a-pulse?cc=BE&lc=dut. [Accessed 03 01 2020].